UNIVERSIDAD DE INVESTIGACIÓN DE TECNOLOGÍA EXPERIMENTAL YACHAY

School of Chemical Sciences and Engineering

TITTLE: "Ni-DOPED Cu-BTC FOR DIRECT HYDROXYLATION OF BENZENE TO PHENOL".

Trabajo de integración curricular presentado como requisito para la obtención del título de Ingeniero en Polímeros

Author:

Zenteno Sanchez Jeremee Paul

Advisor:

PhD Terencio Thibault

Urcuquí, September 2019

SECRETARÍA GENERAL
(Vicerrectorado Académico/Cancillería)
ESCUELA DE CIENCIAS QUÍMICAS E INGENIERÍA
CARRERA DE POLÍMEROS
ACTA DE DEFENSA No. UITEY-CHE-2019-00006-AD

En la ciudad de San Miguel de Urcuquí, Provincia de Imbabura, a los 23 días del mes de agosto de 2019, a las 14:00 horas, en el Aula AI-101 de la Universidad de Investigación de Tecnología Experimental Yachay y ante el Tribunal Calificador, integrado por los docentes:

Presidente Tribunal de Defensa	Dr. DÍAZ BARRIOS, ANTONIO , Ph.D.
Miembro No Tutor	Dra. SOMMER MARQUEZ, ALICIA ESTELA , Ph.D.
Tutor	Dr. THIBAULT TERENCIO , Ph.D.

Se presenta el(la) señor(ita) estudiante ZENTENO SANCHEZ, JEREMEE PAUL, con cédula de identidad No. 1720933033, de la ESCUELA DE CIENCIAS QUÍMICAS E INGENIERÍA, de la Carrera de POLÍMEROS, aprobada por el Consejo de Educación Superior (CES), mediante Resolución RPC-SO-41-No.476-2014, con el objeto de rendir la sustentación de su trabajo de titulación denominado: NI-DOPED CU-BTC FOR DIRECT HYDROXYLATION OF BENZENE TO PHENOL, previa a obtención del título de INGENIERO/A DE POLÍMEROS.

El citado trabajo de titulación, fue debidamente aprobado por el(los) docente(s):

Tutor	Dr. THIBAULT TERENCIO , Ph.D.

Y recibió las observaciones de los otros miembros del Tribunal Calificador, las mismas que han sido incorporadas por el(la) estudiante.

Previamente cumplidos los requisitos legales y reglamentarios, el trabajo de titulación fue sustentado por el(la) estudiante y examinado por los miembros del Tribunal Calificador. Escuchada la sustentación del trabajo de titulación, que integró la exposición de el(la) estudiante sobre el contenido de la misma y las preguntas formuladas por los miembros del Tribunal, se califica la sustentación del trabajo de titulación con las siguientes calificaciones:

Tipo	Docente	Calificación
Presidente Tribunal De Defensa	Dr. DIAZ BARRIOS, ANTONIO , Ph.D.	9.8
Miembro Tribunal De Defensa	Dra. SOMMER MARQUEZ, ALICIA ESTELA , Ph.D.	10,0
Tutor	Dr. THIBAULT TERENCIO , Ph.D.	10,0

que da un promedio de: 9.9 (Nueve punto Nueve), sobre 10 (diez), equivalente a: APROBADO

Para constancia de lo actuado, firman los miembros del Tribunal Calificador, el/la estudiante y el/la secretario ad-hoc.

ZENTENO SANCHEZ, JEREMEE PAUL
Estudiante

Dr. DÍAZ BARRIOS, ANTONIO , Ph.D.
Presidente Tribunal de Defensa

Dr. THIBAULT TERENCIO , Ph.D.
Tutor

Dra. SOMMER MARQUEZ, ALICIA ESTELA , Ph.D.
Miembro No Tutor

ESCOBAR LANDAZURI, ANA MARIA
Secretario Ad-hoc

Hacienda San José s/n y Proyecto Yachay, Urcuquí | Tlf. + 593 6 2 999 500 | info@yachaytech.edu.ec
www.yachaytech.edu.ec

4

AUTORÍA

Yo, **Jeremee Paul Zenteno Sánchez**, con cédula de identidad 1720933033, declaro que las ideas, juicios, valoraciones, interpretaciones, consultas bibliográficas, definiciones y conceptualizaciones expuestas en el presente trabajo; así cómo, los procedimientos y herramientas utilizadas en la investigación, son de absoluta responsabilidad de el/la autora (a) del trabajo de integración curricular. Así mismo, me acojo a los reglamentos internos de la Universidad de Investigación de Tecnología Experimental Yachay.

Urcuquí, septiembre del 2019.

Jeremee Paul Zenteno Sánchez
CI: 1720933033

AUTORIZACIÓN DE PUBLICACIÓN

Yo, **Jeremee Paul Zenteno Sanchez,** con cédula de identidad 1720933033, cedo a la Universidad de Tecnología Experimental Yachay, los derechos de publicación de la presente obra, sin que deba haber un reconocimiento económico por este concepto. Declaro además que el texto del presente trabajo de titulación no podrá ser cedido a ninguna empresa editorial para su publicación u otros fines, sin contar previamente con la autorización escrita de la Universidad.

Asimismo, autorizo a la Universidad que realice la digitalización y publicación de este trabajo de integración curricular en el repositorio virtual, de conformidad a lo dispuesto en el Art. 144 de la Ley Orgánica de Educación Superior

Urcuquí, septiembredel 2019.

Jeremee Paul Zenteno Sanchez
CI: 1720933033

Acknowledgments

For god, family, and friends. For my family that has always been there to support me every day especially my mother who believes and supports me in the good and bad moments. For my friends and the special people who are an excellent company through these years and the good moments that I shared with them. For all the teachers that teach me in every class, especially Thibault Terencio excellent mentor that support and guiding me throughout the last year of this project.

For all of them, thank you so much.

Abstract

Metal Organic Frameworks (MOFs) are novel materials with vast applications such as catalysis, dye adsorption, drug retention, or gas storage.[1] MOFs can retain molecules inside their microporosity or onto its surface due to its 3D structure. One of the main advantages of the MOFs is the chemical diversity present at their surface because they consist of an organic ligand and a metal center. In this case, Copper (II) acts as the metal center and benzene-1, 3, 5 tricarboxylic acid BTC as the organic ligand, to form HKUST-1 (also known as Cu-BTC or MOF-199). Despite the diversity of existing inorganic and organic parts, each MOF usually contains only one type of transition metal. However, the advantage of having two different metals brings usually new properties, for example, in the case of Cu-Ni alloys. The objective of this work is to take advantage of two different metals, namely copper and Nickel, and of the 3D structure of the MOF. Alternatively, in other words, make Ni-doping of the HKUST-1 material, verified both by experimental and theoretical technics. Moreover, finally, test the catalytic activity of this new material, in this case, the direct hydroxylation of benzene to phenol. The Ni-doped material showed to be a better catalyst than the simple HKUST-1.

Keywords

MOF, catalysis, 3D porous materials, oxidation reaction, Ni-doping.
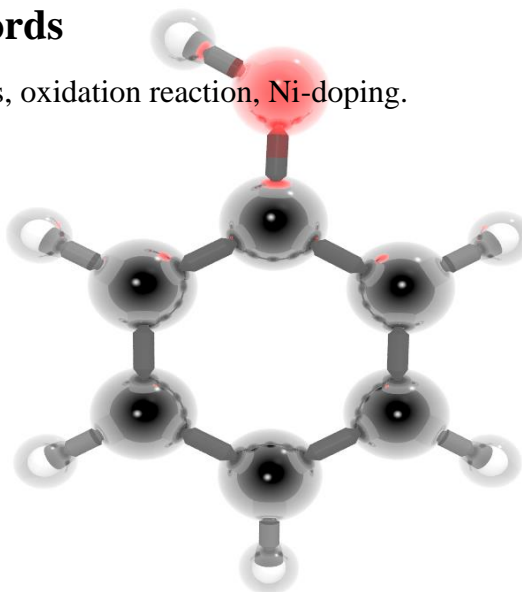
Abstract

La redes metal-orgánicas (MOF por sus siglas en inglés) son materiales novedosos con una gran cantidad de aplicaciones como es catálisis, adsorción de colorantes, retención de drogas, o almacenamiento de gases. MOFs tienen la capacidad de retener moléculas dentro de su micro porosidad o en la superficie debido a su estructura 3D. Una de las grandes ventajas de estos materiales es la diversidad química presente en su superficie porque estos materiales están constituidos por un ligando orgánico y un centro metálico. En este proyecto, Cobre (II) hace de centro metálico mientras que el ácido trimésico (BTC) como ligante orgánico para así formar HKUST-1 (conocido también como Cu-BTC o MOF-199). A pesar de la gran variedad de centros metálicos y ligantes orgánicos que existen actualmente, normalmente cada MOF contiene solo un tipo de metal de transición. Sin embargo, la ventaja de tener dos tipos de metales traería nuevas propiedades al catalizador como es el caso de aleaciones Cu-Ni. El objetivo de este trabajo es tomar ventaja de dos tipos de metales diferentes, en este caso Cobre y Níquel, y la estructura tridimensional de la red metal orgánica. En preferencia, esto quiere decir que se intentara dopar al catalizador HKUST-1 con Níquel, verificando este proceso con técnicas teóricas y experimentales. Finalmente, realizar un test catalítico para analizar la actividad del nuevo catalizador, en este caso la hidroxilación directa de benceno a fenol. El catalizador dopado con Níquel demuestra ser un material más activo que HKUST-1.

Palabras clave

MOF (Red metal-orgánica), catálisis, materiales porosos, estructura 3D, reacción de oxidación, Dopaje con nickel.

Table of contents

This chapter presents the motivation for phenol production, the industrial context of this production, the best current approach and the proposition/objectives of this work.

1.1 Relevance of the topic to industrial process

Phenol

Phenol is an organic compound; alcohol, characterized by the presence of the hydroxyl group linked to a benzene ring. (**Figure 1**) Phenol is used to name an entire family of organic compounds, but the term points to a specific compound also known as benzenol or carbolic acid. Phenol was isolated in 1865 by Joseph Lister, who used it as antiseptic[2]; currently, this compound has a many applications from household[3] products to reagents and intermediates for industrial synthesis.[4]

Figure 1. Schematic(left) and 3D structure (right) of phenol molecule

Due to the presence of hydroxyl functional group in their structure, phenol has similar properties as other alcohols, and it can also participate in the intermolecular hydrogen bonding. Some physical properties of phenols are molecular weight of 94 g/mol, a boiling point of 455 K (more than several hydrocarbons with the same MW), low solubility in water, among others. Its structure influences the chemical properties of phenol; it presents five resonance structures (**Figure 2**) that may give protons. The difference between aliphatic alcohol and phenol lies in the electronic delocalization in the benzene ring of phenol. The acidity of phenols is more than alcohol but lower than carboxylic acid compounds.
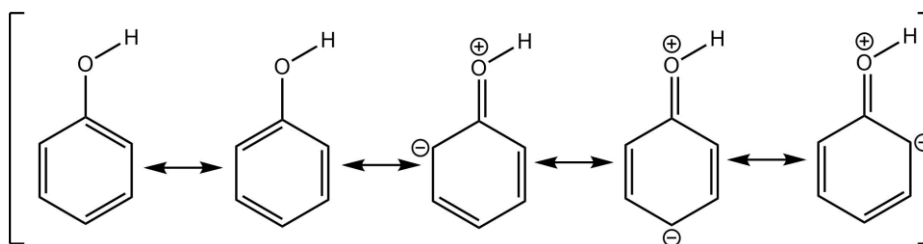
Figure 2. Resonant structures of phenol, these show partial negative charges appearing in ortho and para positions

Phenol is one of the essential commodities in the industry due to its use as a precursor of dyes, polymers, pharmaceuticals, and others[4]. For example, in the polymers industry for the production

of phenolic resins[5]; industrial uses it as conservative additives, adhesives; in the food processing industry as a flavoring agent, colors, and appetizing. (**Figure 3**) Currently, more than 96 % of phenol is producing by the cumene process[6], involving three steps: production of cumene, conversion of cumene to cumene hydroperoxide, and decomposition of cumene hydroperoxide.[7,8] Nevertheless, the cumene process presents some disadvantages in their process that leads to the lower yield of phenol, near to 5%, primarily due to the formation of acetone as a byproduct in the final step with 1:1 stoichiometry. Moreover, cumene hydroperoxide is an explosive intermediate, not environmental friendly. Besides, high pressure, high temperature, and strongly acidic conditions are required.[6]
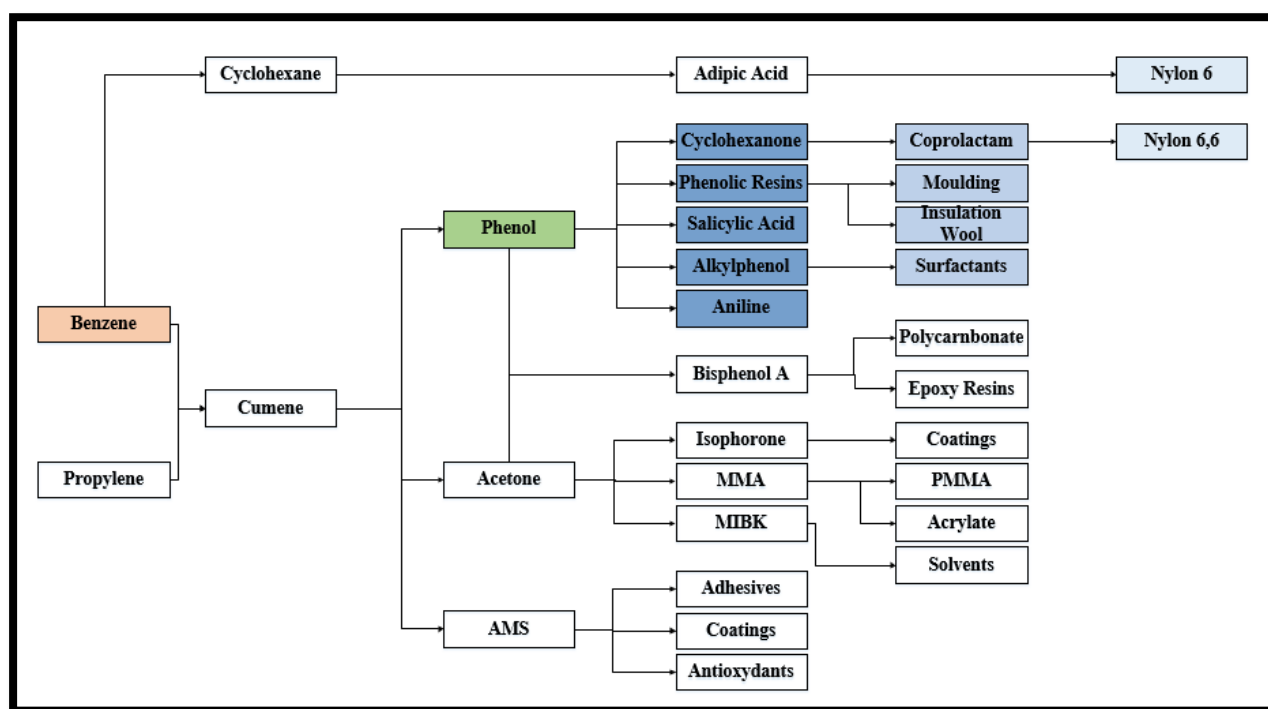

Figure 3. Value chain of phenol

Nowadays, the global production of phenol reaches 10 MMT per year; the largest producers of phenol are the USA and Western Europe, as shown in **Figure 4**. Besides, as shown in this figure, three end products represent nearly 75% of all phenol consumed in the world: bisphenol-A, phenolic resin, and caprolactam.[9]
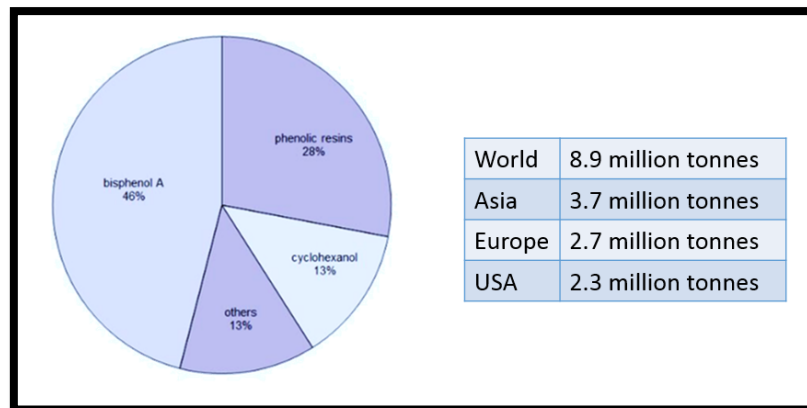
Figure 4. Worldwide production of phenol, and principal end-products.

1.2 Aromatic compounds in Ecuador

The aromatic compounds are present in some final products in the refineries of Ecuador in order to increase the octane number in fuels. The principal component of these components is benzene and other components such as polyaromatic hydrocarbons, benzenoids, and compounds with five polycondensates rings. As an example, the content of benzene in "gasoline extra" is 0.8% vol and 0.95% vol in fuel "gasoline super." In the SARA analysis made in an oil well of Tiputini, C Platform, ITT camp in Ecuador; show that the crude oil presents 30% vol of aromatics.[10]

A couple of years ago, Ecuador proposed a new Refinery called "Refineria del Pacifico," where the first stage consists of the use of xylene, benzene, propylene, ammonia, and ethylene to form products as detergents, plastic resins, textiles, and others. Specifically, the products desired from benzene was chlorobenzene, styrene, polystyrene, acrylonitrile butadiene styrene (ABS), styrene butadiene rubber (SBR), and linear alkyl benzene (**Figure 5**).[11]
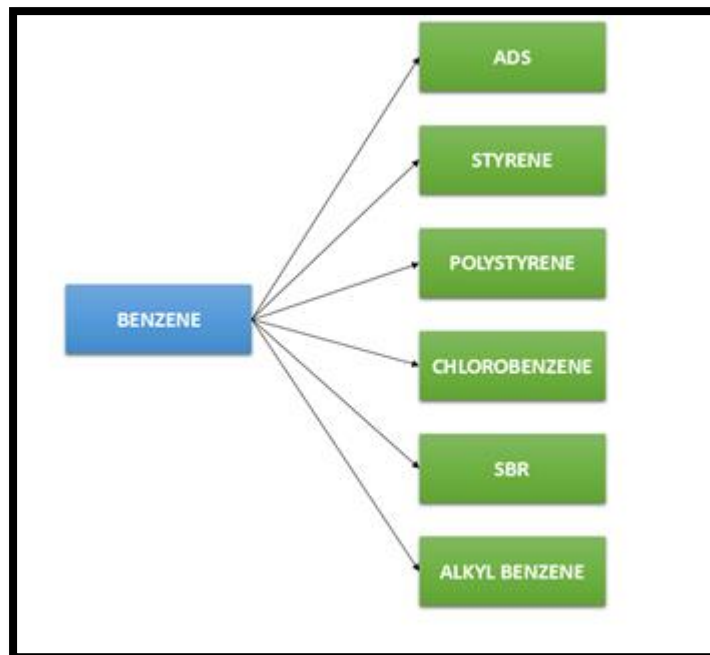
Figure 5. Phases of production using benzene as starting reagent

1.3 Oxidation of Benzene to Phenol

Oxygen is one of the most abundant elements on Earth with more than 50%, and oxygen reactions represent great importance in our lives ranging from biological reactions in animals and plants to catalytic reactions in an industrial process. Nevertheless, oxidation catalysis currently suffers from several disadvantages such as low conversion (production of undesired byproducts), the small activity of catalysts, high cost of production, unfriendly to the environment, and others. The oxidation reaction of paraffin and aromatic hydrocarbons to alcohols and phenols are two reactions that have attracted the interest of several researchers, looking for active, selective, and cheap catalysts.

Phenol was firstly isolated from coal tar in 1834 and called "carbolic acid." The interest and different applications of this compound throughout history gave rise to the development of several synthetic phenol preparations. At present, several processes to produce phenol exist with different advantages and disadvantages based on the raw materials, catalysts, operational conditions used, or the byproducts formed. It is crucial to take into account all of these considerations to choose the best process with a maximum yield of phenol. The process to produce phenol are:[12]

- Cumene process

- Benzene sulphonation
- Oxidation of Toluene
- Phenol from coal
- Toluene- Benzoic acid

Cumene Process: or Cumene peroxidation, constitutes three steps: the Alkylation of benzene to cumene, cumene oxidation to cumene hydroperoxide (CHP), and decomposition to phenol and acetone as a byproduct. This process was developed in 1942 in the former Soviet Union, and in 1949 the first industrial plant started to work. The process starts with the formation of an emulsion of cumene and sodium carbonate solution; sodium stearate acts as an emulsifier. The emulsion is oxidized in the reactor at atmospheric pressure with air, using a catalyst of copper or manganese salt during 3-4 hours at a temperature between 160-210 ℃; cumene hydroperoxide formed. Then, the product decomposed by acid catalyst (commonly sulphuric acid 5-50% wt) at a specific pressure and a temperature between 45-65 ℃; as a result, phenol, cumene, and acetone produced. The final steps consist of the separation of acetone, phenol, and the recycling of cumene to the first step of the process. The figure below shows the reaction mechanism.[13]
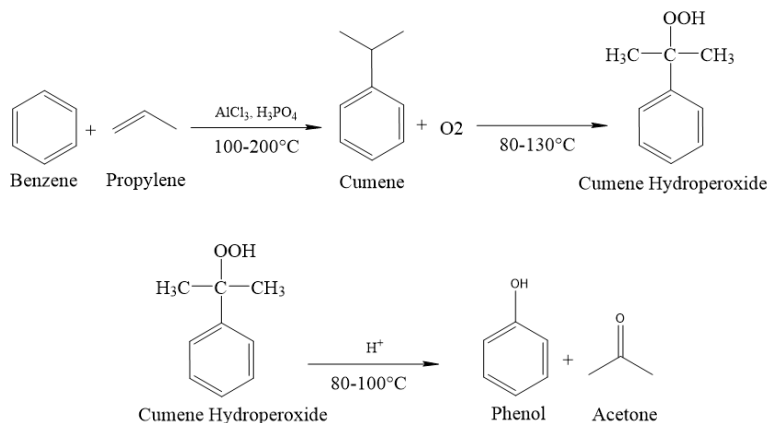
Scheme 1. *Mechanism reaction for cumene process.*

Benzene sulphonation: This was the first method taken to industrial scale in 1899, it has been used for 80 years in the industry but has many disadvantages such as a low yield of phenol, aggressive reagents, a large amount of waste sodium sulfite, and others. As a result, this method is no longer use in the industry.
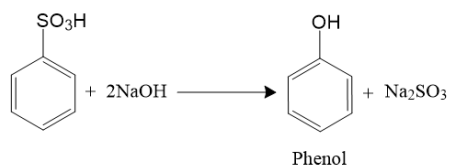
Scheme 2. Mechanism reaction for benzene sulfonation

Oxidation of toluene: There are two types of reaction in this method: Alkaline hydrolysis, also known as the Dow process, and the Rasching-Hocker process. The first one was brought at an industrial scale in 1924 by Dow chemical in the U.S.A. The reaction consists of the chlorination of benzene with ferric chloride as the catalyst at temperatures between 25-50 ºC. Then, chlorobenzene is hydrolyzed with sodium hydroxide at 300-390 ºC and 300 atm to form phenol and sodium chloride. The second one also consists of the formation of chlorobenzene, but in that case, benzene is oxychlorinated in the presence of hydrochloric acid, oxygen obtained from air, and catalyst of iron and copper under atmospheric pressure used. Then, chlorobenzene is hydrolyzed with a catalyst to produce benzene and hydrochloric acid.
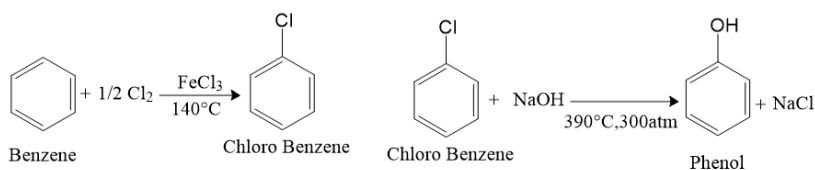
Scheme 3. General mechanism for toluene oxidation.

Phenol from coal: This process suffers from significant drawbacks such as the high cost of operation (due to the energy necessary), equipment (7 columns), dangerous to the operational staff.

Toluene- benzoic acid process: It is the only method that does not use benzene as raw material. This method consists of two reactions. The first reaction is the oxidation of toluene to benzoic acid in the presence of a cobalt catalyst at 140° C and 2 atm. The second reaction presents some difficulties such as degradation of the catalyst and low selectivity; it consists of two reactions in series, the oxidation of benzoic acid with oxygen and catalysts of copper and magnesium salts, and finally hydrolyzed to phenol and carbon dioxide as a byproduct. At present, this method is using, but only represents 5% of the world phenol production.[12,14]
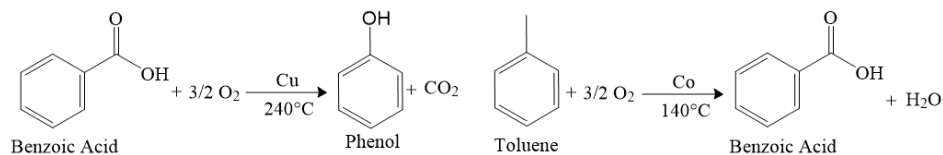
Scheme 4. *Mechanism for Toluene-benzoic acid process*

1.4 Cumene to Phenol Industrial Processes

As mentioned before, the cumene process consists of three steps: benzene alkylation to cumene, cumene oxidation, and decomposition of cumene peroxide to phenol and acetone. At the begining of the 20th century, phenol was synthesized primarily by two methods: benzene chlorination and sulfonation process, providing to the resin industry. Since 1940 to present, more than 90% of phenol production has made via the cumene peroxide process. As a result, several technologies have emerged in order to improve phenol/acetone quality, production yield, cumene conversion, among others. Presently, some technologies represent in the area of the cumene peroxidation method as Sunoco/UOP, ILLA Internationa, KBR, and GE/Lammus. Sunoco/UOP phenol process produces phenol and acetone with a high level of purity, using oxygen from the air. Has low feedstock consumption without tar cracking, no acetone recycling to cleavage section, simplified neutralization, efficient purification, low overall capital, and production costs. ILLA´s phenol technology uses the same manufacturing process as the other licenses. However, only ILLA International does scientific research intending to improve the cumene process.[6]
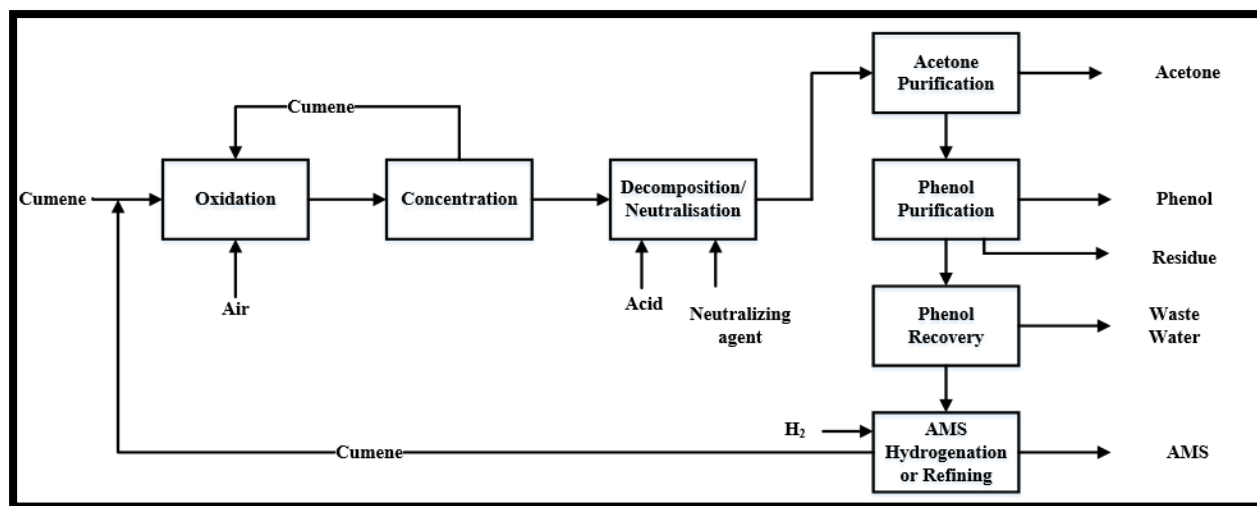
Figure 6. *BDP for Sunoco/UOP license.*

ILLA International Process

The technology involved in the ILLA phenol process has three key steps to ensure the quantity and quality parameters: cumene oxidation, cumene hydroperoxide (CHP) decomposition, and purification of phenol. The other steps of the process are similar to the other licenses.[6]
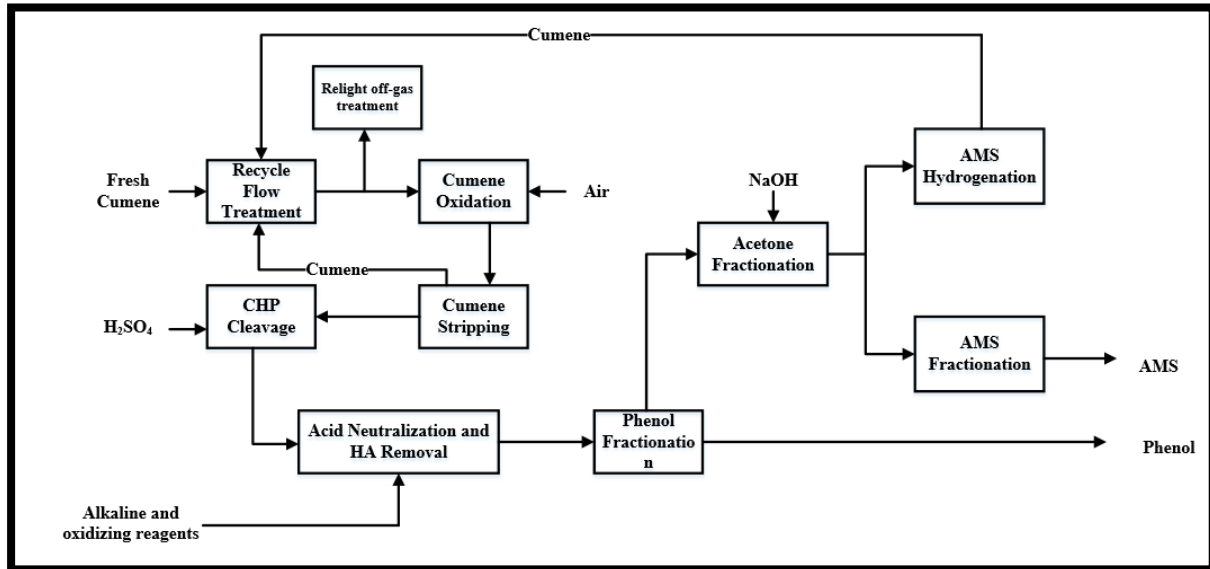
Figure 7. ILLA license BDP

Cumene oxidation: The cumene oxidation reaction follows the radical chain mechanism, uses air oxygen to form cumene hydroperoxide; the recycle streams are treated with an alkaline agent to maintain the pH values in the general requirements and the addition of neutralizer in oxidation product minimized the effect on the reaction rate increasing the cumene hydroperoxide rate and selectivity. The cumene oxidation is between 95.5-95% mol and a cumene conversion of 20-22% mol. Several advantages of this process are the reduction of the presence of inhibitors, stabilization of pH values, control of heat and concentration of oxygen in the reactors, hold the best operational conditions based on the kinetic model.

Off-Gas Purification: The sorption methods that used carbon materials for cleaning gases are not using for several disadvantages like methanol sorption and lifetime. This step uses two types of zeolites to remove methanol and cumene; later, desorption is producing with vapor. The lifetime of zeolites used in this process is about five years, in comparison with carbon that is only 1.5 years.

Cleavage or CHP Decomposition: For the first stage H_2SO_4 catalyst is used, for the second one NH_4HSO_4 mild acidic catalyst used to reduce the formation of byproducts through the process

(90% mol AMS yield). The stage has acetone recycle stream to improve final product quality and lower environmental impact.

Fractionation: The CHP cleavage product stream has hydroxyacetone (HA), acetone, carbonyls, cumene, AMS, phenol, and other components; the stream is directing to phenol and acetone fractionation. The first column separates acetone, cumene, AMS, and light components are separated, then, acetone recuperation and AMS hydrogenation step proceeds. The process has lower steam consumption and adjustable control of the column conditions.

AMS Hydrogenation and Production: AMS hydrogenation process carries out a high-level AMS to cumene conversion that is recycling to the oxidation step. This step proceeds at a lower level of hydrogen partial pressure. AMS production involves several fractionation columns that produce 99.5% of pure AMS products. This process depends if the consumer prefers AMS as a final product.

Phenol Treatment: This process is essential to the final quality of phenol product; the objective is to remove all of the minor organic compounds by binary catalysts, zeolites in one case. The catalysts have to convert the carbonyls and HA products.[15]

1.5 One-step benzene oxidation

Direct oxidation of benzene could be the easiest way to produce phenol, avoiding several unit operations, and reducing the number of catalysts used in the process. Benzene can be oxidized by air, but phenol is also oxidized and even more quickly than benzene, thus producing byproducts such as hydroquinone, water, and carbon dioxide. The conversion percentage is meager and presently is not yet used for commercial production of phenol. For this reaction, oxygen, hydrogen peroxide, and nitrous oxide have used as oxidizing agents.[15–20]
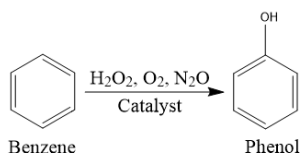
Scheme 5. Direct oxidation of benzene to phenol with different oxidizing agents under the activity of some catalyst

The oxidation using H_2O_2 produces water as a theoretical byproduct.[21,22] The catalysts used for this reaction are common transition metals $M^{n+}/m^{(n-1)+}$. The conversion could be more than 30% and 95% of selectivity with titanium-based catalysts. Meanwhile, with O_2, the selectivity can reach

more than 90% but low values of conversion. Direct oxidation with nitrous oxide is proceeded in the gas phase at 300-450°C, atmospheric pressure in the presence with zeolites as the catalyst. The conversion reached is 40% and selectivity 95% and byproducts formation as carbon dioxide, water, and hydroquinones.

Nitrous oxide is the component of off-gas from the production plant of adipic acid. However, a plant with nitrous oxide has to be near to the adipic acid plant to avoid the transport and storage of the gas. The mechanism remains unclear, but two ideas are proposed; one assumes that nitrous oxide dissociates, at low temperature, into N_2 and O, resulting in benzene oxidation, and the other attributes the catalytic activity to surface acidity.

Alphox process

The direct oxidation process to phenol by nitrous oxide as an oxidizing agent and zeolites as the catalyst as a new way of commercial synthesis was developed by Solutia Inc and BIC, called AlphOx. The operation conditions of the pilot plant shown in table 1. The process only uses an adiabatic reactor to realize the reaction. This process has several advantages in contrast to the cumene process: no intermediates and acetone formation, and only one-step reaction. As mentioned above, the problems are the availability of nitrous oxide for the process and its cost, also, the fast deactivation of the catalyst by the accumulation of phenol inside the pores and the consequent formation of coke.[23]

Table 1. AlphOx process characteristics

Catalyst	Fe-ZSM5
Phenol productivity (kg/kg cat h)	0.4
Benzene conversion to phenol (mol%)	97.98
N2O conversion to phenol (mol%)	85
Temperature of operation (°C)	400-450
Contact time (s)	1-2

1.6 Objectives of the project

The principal objective of this project is to develop a new catalyst efficient for the direct benzene oxidation to produce phenol.

The project is logically subdivided into 3 specific objectives:

> **1) Synthesize the HKUST-1 catalyst with the metathesis method**

> **2) Doping the material with Nickel using three different approaches:** *ship in bottle, bottle around the ship,* **and** *one step*

> **3) Test the efficiency of this new catalyst for the direct hydroxylation of benzene to phenol.**

2 Chapter 2: State-of-the-art

This chapter presents the state-of-the-art of the materials, specifically of the Metal Organic Frameworks, their application in catalysis and their relevance to benzene oxidation.

2.1 Porous materials

2.1.1 Porous Materials

Porous materials are materials built with a specific 3D structure that lets appear free space called pores. Porous materials possess a low density and a large specific surface allowing the entrance of other molecules. The principal properties discussed of porous materials are pores shapes, pores size, pore size distribution, specific surface. A surface is generally a physics domain that is known to bring particular properties (physisorption, chemisorption). In the case of porous material, particular properties are coming from the confinement effect inside the porosity and the lack of neighboring atoms in comparison to the bulk material. Consequently, porous materials mainly used for adsorption and catalysis applications. Common examples of such porous materials industrially used are activated carbon, silica, zeolites, and others.

Depending on the diameter of the pores inside the material, different categories can be defined according to IUPAC: microporous (pores<2nm), mesoporous (2nm<pores<50nm) and macroporous (>50nm). A second classification can be done according to their crystallinity: crystalline materials possess atoms periodically spaced which confers the materials the property of displaying a discrete XRD diffractogram. Amorphous materials show an unordered structure, neither a structure at a short-range nor at a long-range. A third classification can be based on the nature of the atoms constructing the structure, either organic or inorganic.

2.1.2 Metal Organic Frameworks

Metal Organic Frameworks (MOF) produced by bonding an organic linker and a metallic center. For this reason, MOF is neither purely organic nor inorganic but pertains to the hybrid category. The linking of these two building units (organic and inorganic) produces different coordination modes, depending on the symmetry and coordination number of the linker and metal center; it means that the structure of the MOF is affected by a couple of factors of linker such as the geometry, shapes, functional groups.[24,25].

The crystalline structure of the frameworks could be 1D, 2D, or 3D, generating high surface area and pore volume. This architecture of the MOF depends on the type of organic unit, whose could be ditopic or polytopic, linked with metal-containing units (secondary building units (SBU)). Some of the usual structures present in the MOFs are linear, trigonal, tetrahedral, square planar, trigonal pyramidal and others.[26] Additionally, an extraordinary variety of organic and inorganic parts exist, generating more than 20 000 different MOFs

2.2 HKUST-1

HKUST-1 also called MOF-199, or Cu-BTC is one of the most studied MOFs due to its 3D structure with a different distribution of porous sizes with high pore volume and surface area; the unsaturated copper (II) sites in the structure can bind water, ethanol, and other molecules easily. HKUST-1 also known as MOF-199 or Cu-BTC (BTC means the linker 1,3,5 benzene tricarboxylate) was synthesized for the first time in 1999 by Chui and collaborators in the Hong Kong University of Science and Technology[27]. This MOF formed by copper Cu(II) that acts as the metal site and the organic linker benzene-1,3,5-tricarboxylic acid (also referred to as trimesic acid) commonly synthesized by solvothermal method, electrochemical method, and microwave-assisted method [28]. The Cu-BTC structure consists of a monomeric unit with a dicopper cluster named Paddlewheel (**Figure 8**) and a copper-copper distance of 0.263 nm, where, four oxygen atoms from four linkers coordinate to copper.[28] Also, this MOF is a crystalline material; the space group is a face-centered crystal lattice with Fm-3m Symmetry.[1,29]
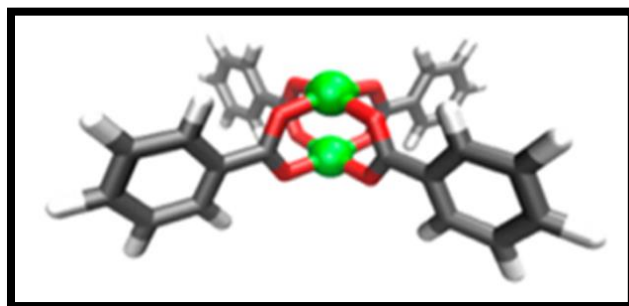
Figure 8. Paddlewheel cluster of HKUST-1 MOF. Green: Cupper, red: oxygen

Methods of synthesis

Since the first synthesis of MOF in 1999 to now, several methods of synthesis have developed. These methods have variations in the compositional and process parameters that lead to changes

in the final product characteristics such as particle sizes, size of porous, shape of the crystal, among others. It means that different synthesis methods can influence the properties of the material obtained, such as adsorption of the products, catalytic behavior, pore size distribution, and others. Moreover, several researchers focus on the scale-up reaction of MOFs, and even some patents have created due to the novel features of this material. However, it should be considered potential problems in the industrial production of MOF such as sustainability, availability and high costs of linkers or solvents, as well as appropriated reaction conditions, but is not limited.[25,30,31]

The conventional methods of synthesis are:

- Solvothermal synthesis
- Mechanochemical synthesis
- Electrochemical synthesis
- Microwave or ultrasound-assisted synthesis

Solvothermal synthesis: The reaction of the organic linker, metal salt, and solvent or mix of solvents, takes place commonly into an autoclave under pressure over 1 atm, the temperature depends on the solvent selected (usually corresponding to the solvent boiling point), the concentration of reactants, and pH. **Mechanochemical synthesis:** Mechanical energy induced into the reaction system promoting chemical reaction (decomposition, ion exchange, oxidation-reduction, among others) and physical phenomena to produce MOFs; the reaction occurs without the presence of a solvent[30]. **Electrochemical synthesis:** This process avoid the presence of anions such as nitrate, perchlorate, and chloride that contaminate the framework of MOFs. Instead of the use of metal salts, metal ions in anionic solution are feed continuously in the reaction media that contains organic linker dissolved.[32] **Microwave or ultrasound-assisted synthesis:** The mixture with the metal center and linker receive energy by electromagnetic waves, commonly the frequency is between 300 MHz to 300 GHz in the microwave method, meanwhile, in the ultrasound-assisted method the cyclic mechanic vibrations supplied to the system are between 20 kHz to 10 MHz. This synthesis consists of low time reaction in contrast to the other ways of synthesis, minutes.[33]

2.3 MOFs as catalysts

One of the advantages of MOFs is that it can be specifically designed depending on the final catalytic process.[34] In addition to the design of the MOF itself, specific characteristics of these

materials such as high surface area, significant pore volume (even tunable), uniform catalytic sites through the structure, makes it an ideal support for catalysts in their surface or pores features.[35] Some MOFs have demonstrated to possess good Lewis acid sites due to the transition metal of their structures. This particular point is, however, MOF-dependent as the majority of them possess metals with a complete coordination sphere, HKUST-1 being an exception. Another approach is the modification of the organic linker in order to bring new functional groups. Several applications of MOFs as catalysts showed in the table. [30,36] Although several researchers were carried out, the complete understanding of catalysis in MOF is still at an early stage and would surely increase in the future.[37] It has been reported that HKUST-1 has following characteristics a)pores diameter ranging from 6 A to 10 A, b) water or solvent molecules coordinated to the Cu (II) are easily removed by thermal o chemical treatment, and c) this exposed open metal sites that can act as Lewis acid catalysts.[30,36,38,39]

2.4   Doping material as a strategy for catalysis

Addition of nanoparticles into MOFs

Nevertheless, MOFs present limiting characteristics such as low chemical, thermal stability, and electrical conductivity; it means a problem in practical applications.[40] These problems initiate the need for increasing the functional properties of MOFs, as solutions some works present the incorporation of functional molecules as organic compounds, inorganic compounds, and biological molecules with the aiming of improving some weak properties of MOFs.[41–43] As shown in Figure 9, there are three different paths to encapsulate functional molecules into MOfs[44]:

a) "ship in bottle"

b) "bottle around the ship"

c) "one-step" synthesis
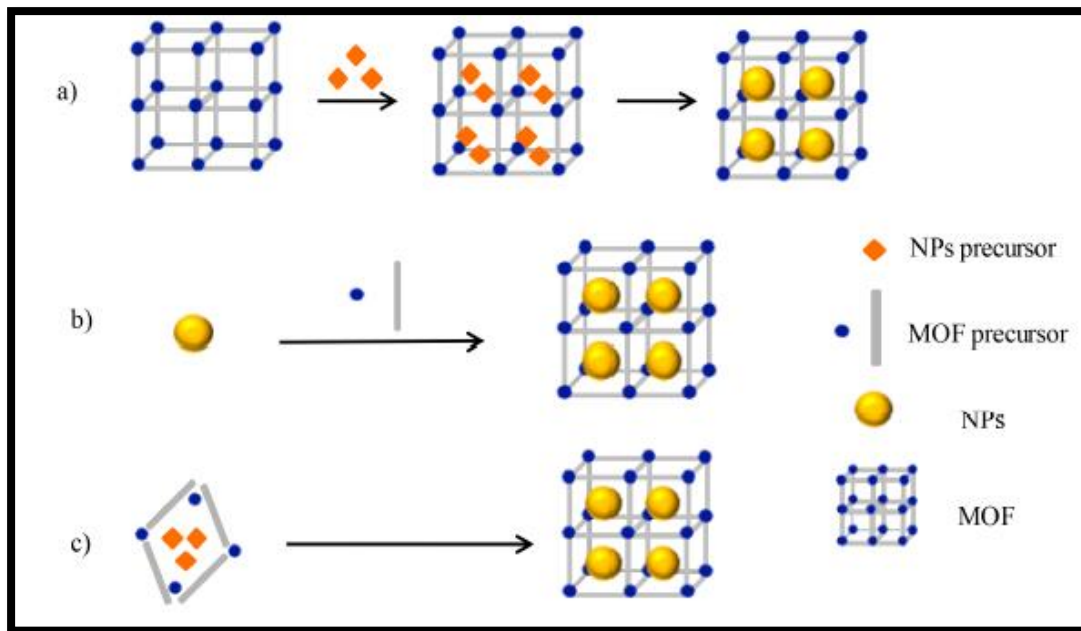
Figure 9: Schematic view of the different approaches for doping a MOF[44]

The first one consists of post-synthesis encapsulation of metal nanoparticles (NPs) into MOFs; the process involves the addition of the NPs precursor into the structure of MOFs, followed by some treatment to obtain the NPs encapsulated into MOFs structure. The method " bottle around the ship" has two steps, first, the synthesis of the nanoparticles, second, the addition of the synthesized NPs into the MOF precursor; getting the growth of the MOF framework around nanoparticles. The last method involves the addition of the MOF and NP precursors in one solution, thus attained the simultaneous growth of both.[44]

2.5 Hydroxylation of benzene with HKUST-1 based materials

Cu-BTC MOF, due to its features as high volume pore, large surface area, chemical, and thermal stability makes it a right candidate for catalysis. HKUST-1 when it is thermal o chemical activated, water leaves the copper (II) sites that act as Lewis acid catalysts; this material has been reported used as heterogeneous catalyst or catalyst support in catalytic reactions such as hydrogenation, oxidation, transesterification, and others.[45] Only two works made by Liu and collaborators[46] have used Cu-BTC MOF as the catalyst for direct oxidation of benzene to phenol; using benzene, H_2O_2 as the oxidizing agent, and acetonitrile at 60 C.

The results of both works shown in **Table 2**. These works suggest that HKUST-1 can act as an excellent catalyst in the reaction with high selectivity to phenol but low yield, and high yield but low selectivity to phenol, depending on the reagents uses in the synthesis[28] and activation[46] of MOFs. The byproducts formed in this reaction are benzoquinone, catechol, and hydroquinone.[47,48]

Table 2. HKUST-1 results as catalyst for oxidation of benzene to phenol.

Phenol selectivity (%)	Yield (%)	TOF/h	Ref
52.6	16.6	16.2	28
88.6	1.7	1.7	
53.3	36.5	35.1	46
77.0	9.5	9.3	

3 Chapter 3: Methods

This chapter makes a brief description of the different technics of characterization used in this project to analyses the catalysts obtained.

3.1 X-Ray Diffraction (XRD)

The XRD technique discovered by von Laue in 1912, is used to characterize the phases present in solid catalysts, giving information about the structure of the matter, atoms ordering, and spacing.

Fundaments of the technique

The X-Ray is electromagnetic radiation with a short wavelength produced by the high-energy electron braking or electronic transitions of electrons. The X-Ray has wavelengths between 10 exposant -5 to 100 A. The interaction of X-Ray with the matter exists in two processes.

1. Some photons of the incident beam deviated without losing energy; photons constitute the scattering radiation precisely with the same λ (wavelength) as the incident radiation.
2. The photons may get a series of inelastic collisions when hitting the target and this energy increases the temperature of the sample or produce fluorescence

This technique is based on the regular, repetitive, and organized distribution of the atoms or molecules that are part of the solid; where the constituents and the distance between them are the same magnitude order as the wavelength of the incident beams. When the X-Ray beam generated and directed to a flat sample placed at a fixed angle, the intensity of diffracted radiation (resulting from the interaction between solid and beam) is in the function of the distance between the crystal planes that are part of the structure and diffraction angle θ.

In the diffraction, the scattered rays that are in phase proceed a constructive interference; meanwhile, those who do not in phase induces a destructive interference. For constructive interference, Bragg Law comes into play.

$$n \cdot \lambda = 2 \cdot d_{hkl} \cdot sen\,\theta$$

Where **θ** represents the diffraction angle in degrees, **d$_{hkl}$** is the distance between crystal planes in angstrom (Å), and **n** is the whole number that represents the re-flexion order. The intensity

of the diffracted beams through a crystal is related to the kind of atom present in the crystal and its location in the unit cell. The interplanar distance **d** can be calculated from the angle **θ** where the diffraction peak appears with **λ** known.

Experimental conditions

The XRD analysis has been made in a diffractometer PANalytical brand model EMPYREAN, working with the configuration θ-2θ. Equipped with an X-Ray tube of copper (Kα radiation λ= 1.54056 A°) at 45kV and 40 mA. The measurements made in quadruplicate. The conditions of the measurements:[49]

Table 3. XRD conditions.

Configuration:	Start angle(°):	Step size (°):	Net time per step(s):
Spinner	5.0000	0.0167	40.05
Scan Mode:	**End angle (°):**	**Time per step (s):**	**Scan speed (°/s):**
Continuous	90.0030	40.05	0.000417

3.2 Surface area determination, BET method

This technique used for solids characterization, the name BET came from the acronym of the authors (Brunauer, Emmet, and Teller) of the particular equation used to calculate the specific surface of catalyst or porous solids. This parameter expresses the relation between the total area and weight of catalyst in a square meter of surface per gram of catalyst (m^2/g).[49]

Fundaments of the technique

The BET method uses the principle of physisorption of inert gases, nitrogen; in this case, to variate the relation between the partial pressure of nitrogen and its vapor pressure at the temperature at which nitrogen is in the liquid state. Besides, with the appropriate calculations are possible to determine the distribution of the porous in the mesoporosity camp.

The BET theory is based on the following assumptions:

1. Adsorption of the adsorbate produced in the overlapping layers of molecules.
2. It does not exist preferential adsorption of adsorbate at any point of the surface.
3. The adsorbed molecules do not interact between them.
4. It supposed a determined mechanism for the first layer, and other for the following layers.

The calculation based on the determination of gas volume required to form a monolayer on the surface of solid. The graphic representation of BET isotherm in linear form utilized:

$$\frac{P}{V \cdot (P_o - P)} = \frac{1}{V_m \cdot C} + \left(\frac{C-1}{V_m \cdot C}\right) \cdot \frac{P}{P_o}$$

Where:

P_o: Saturation pressure of the adsorbate at experimental conditions (-196°C and 1atm).

V: Volume of adsorbed gas at normal conditions (1atm and 0°C) at partial pressure P of adsorbate.

V_m: Volume of gas required to form a monolayer.

P/P_o: Partial pressure

C: Constant related to the net adsorption energy by the equation:

$$C = e^{\left(\frac{E_1 - E_2}{RT}\right)}$$

Where:

E_1: Adsorption heat of the first layer.

E_2: Condensation heat.

R: Ideal gases constant.

T: Absolute temperature.

Then, the specific surface can be calculated by:

$$S_g = \frac{V_m \cdot N_o \cdot \sigma}{V \cdot W}$$

S_g: Specific surface (m^2/g).

V_m: Volume of gas required to form a monolayer (mL)

V: Molar volume (ml/gmol)

N_o: Avogadro number

σ: Area occupied by each molecule of nitrogen adsorbed.

W: Weight of the sample (g)

It should be noted that the BET model is a multilayer model, adequate for porosity in the range of mesoporosity. In our case, HKUST-1 is a microporous material, and MOFs materials, in general, are well known to follow the Langmuir model (mono-layer). However, the majority of specific surface are reported using the BET model. We will also use this model for the sake of comparison.

3.3   UV-vis/nIR Spectra

3.3.1   UV-vis spectroscopy

The spectrophotometry UV-Vis implies spectroscopy with photons in the ultra-violet and visible radiation range. In this range of the electromagnetic spectra, the energy given can result in electronic transitions from one orbital to another unoccupied. This technique based on the transition from a ground state to an excited state upon light absorption.

Fundaments of the technique

The spectrophotometry UV-Vis is commonly used in the qualitative determination of solutions of metallic transition ions, organic compounds, and solids. The metallic transition ions absorb visible light due to the electrons can be excited from an electronic state to another (typically d-d transition). The color of this solution could be affected by the presence of other species such as anions or ligands. The organic compounds solutions, especially those that have a high level of conjugation, also absorb light in the range of visible electromagnetic spectra and UV (typically π-π^* transition). The dissolvent for these solutions can be ethanol or water, depending on the solubility of the organic compound, due to some organic solvents have a significant UV absorption. The polarity and pH of dissolvent can affect the adsorption of the spectra of an organic compound; more generally, the temperature, concentration of electrolytes, presence of interfering substances, pH of the solution, and nature of dissolvent are some factors that can influence in the absorbance spectra of the samples.

The Beer-Lambert law is used to determine the concentration of absorbing species in solution from the spectrophotometry UV-Vis. Using the following equation:

$$A = - \log_{10}\left(\frac{I}{I_0}\right) = \varepsilon \cdot c \cdot L$$

Where:

A: Absorbance measured.

I: Transmition intensity

ε: Molar absorptivity or extinction coefficient (constant)

L: Route length through the sample

c: Concentration of the absorbent species

This law does not work as a universal relation for the concentration and absorption of all substances, as big size molecules.

The instrument used, spectrophotometer UV- Vis, measures the intensity of the light that passes through the sample (I), and compares with the intensity of the light before it passes through the sample (I_0). The relation I/I_0 called transmittance, expressed in percentage (%T), and absorbance (A) based on the transmittance with the following equation:

$$A = - \log(\%T)$$

The parts of a spectrophotometer are:

1. Source of light (incandescent bulb for visible wavelength or deuterium lamp for UV).
2. Sample holder.
3. Diffraction grading used to separate the different wavelengths of light.
4. Detector

The UV-Vis spectra is a graph of light absorbance vs wavelength (λ) in UV or visible light range.

3.3.2 Near Infra-red

The general principle of measurement is similar to UV-vis experiments. The main difference lies in the effect that has the light on the matter for the wavelength corresponding to near-IR. In the range of middle-infrared, the absorption of light induces the vibration of different groups through stretching, bending, twisting, and other modes. In the near-IR range, only the harmonic or combinations of the vibrations observed in mid-IR are observed. As such, it is possible to identify the bands corresponding to water quickly. Near Infra-red is primarily used for control of the quality of products.

3.3.3 Diffuse reflectance spectroscopy

Whether we would like to measure UV or nIR, the most common way is to measure directly the light which is going through a sample as described before (absorbance or transmittance). This method is perfectly adequate for measuring liquids, or transparent solid layers, of different concentration which absorb only partially the light. The problem is how to measure solid which are not transparent, like for example a powder? For solving this problem, the diffuse reflectance technics have developed. Instead of direct absorption, the light reflected in different directions on each particle constituting the solid. The central physical concept behind this technic is the diffuse reflection, which is different from the specular reflection (only at one angle). This technique provides the measurement of the surface and penetrates slightly inside the material.[50] The accessory used for this kind of measurement is called Praying Manthis and collect the diffused reflected light through a set of mirrors. The spectra measured in reflectance and the signal can further transformed for quantitative purposes through, for example, the Kubelka-Munk equation.
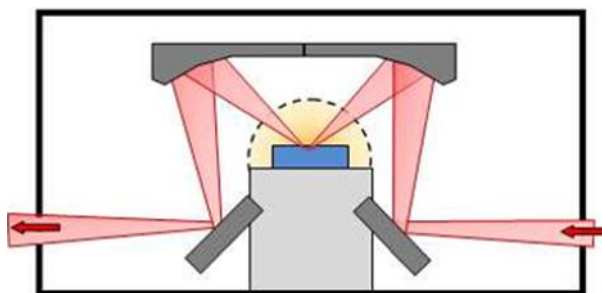
Figure 10. Schematic view of diffuse reflectance apparatus.[50]

3.3.4 Experimental conditions

The spectra recorded on a PerkinElmer Lambda 1050 apparatus. The liquid samples measured in a quartz cuvette of 1 cm in absorbance mode. The solid samples measured on the same apparatus using the Praying Manthis accessory in reflectance mode. The signal then processed using the Kubelka-Munk transformation.

4 Chapter 4: Results and discussion

This chapter exposes and makes a critical analysis of the results obtained concerning the three parts of this project: material (HKUST-1) synthesis, doping with Nickel, test this material for catalysis (benzene oxidation)
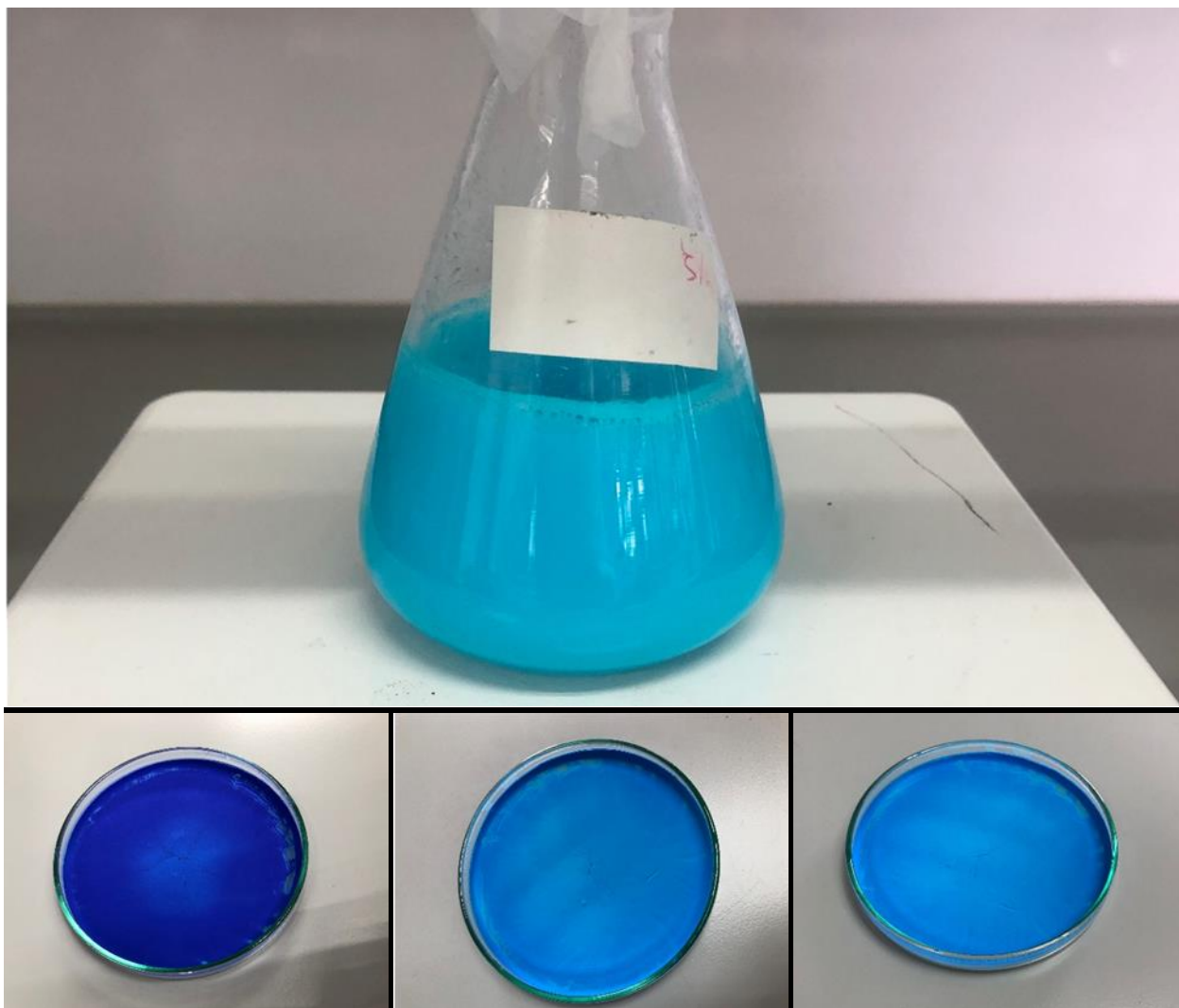
4.1 HKUST-1

4.1.1 Synthesis method used

As highlighted before in the state of the art part, Cu-BTC usually synthesized through a solvothermal approach,[27,51–53] which is also the most common way to synthesize MOFs in general. However, a new method of synthesis proposed recently[1] based on much more mild conditions, which makes it a fascinating approach. The synthesis of Cu-BTC material in this work follows this "metathesis" method. The method consists of the next steps:

1. *Organic linker preparation:* 2.0 mmol (0.25 g) of BTC and 0.35 g of NaHCO$_3$ was dissolved into 100 mL of deionized water: this solution was stirred for one hour.

2. *Precursor salt:* 3.0 mmol (0.43g) of copper nitrate was dissolve in 20 mL of ethanol.

3. *Mixture*: Precursor salt was added gradually drop by drop into the first solution. The mixture obtained was stirred at room temperature for 12 hours.

4. *Separation and drying:* The solution was separated by centrifugation, washing three times with ethanol and drying at 373K for 4 hours and 333K for 8 hours.

Figure 11 shows the blue solution during the synthesis. When taken out of the oven, the powder MOF has a characteristic dark blue color of its activation (free copper sites). Upon contact with ambient humidity, the sample takes rapidly (within a minute) a light blue color, particular when water molecules coordinate to the copper sites.

Figure 11. a) Solution during synthesis of HKUST-1.
b) Solid HKUST-1 obtained at the end of drying process directly taken from oven, c) after 1 min d) after 2 min in air

4.1.2 UV-vis characterization of the obtained material
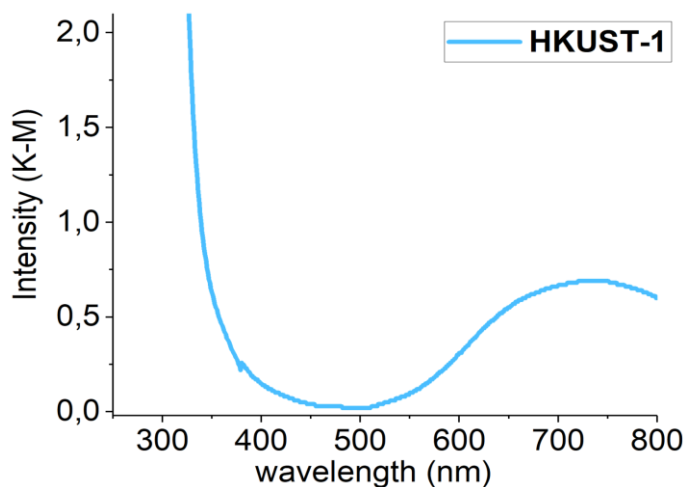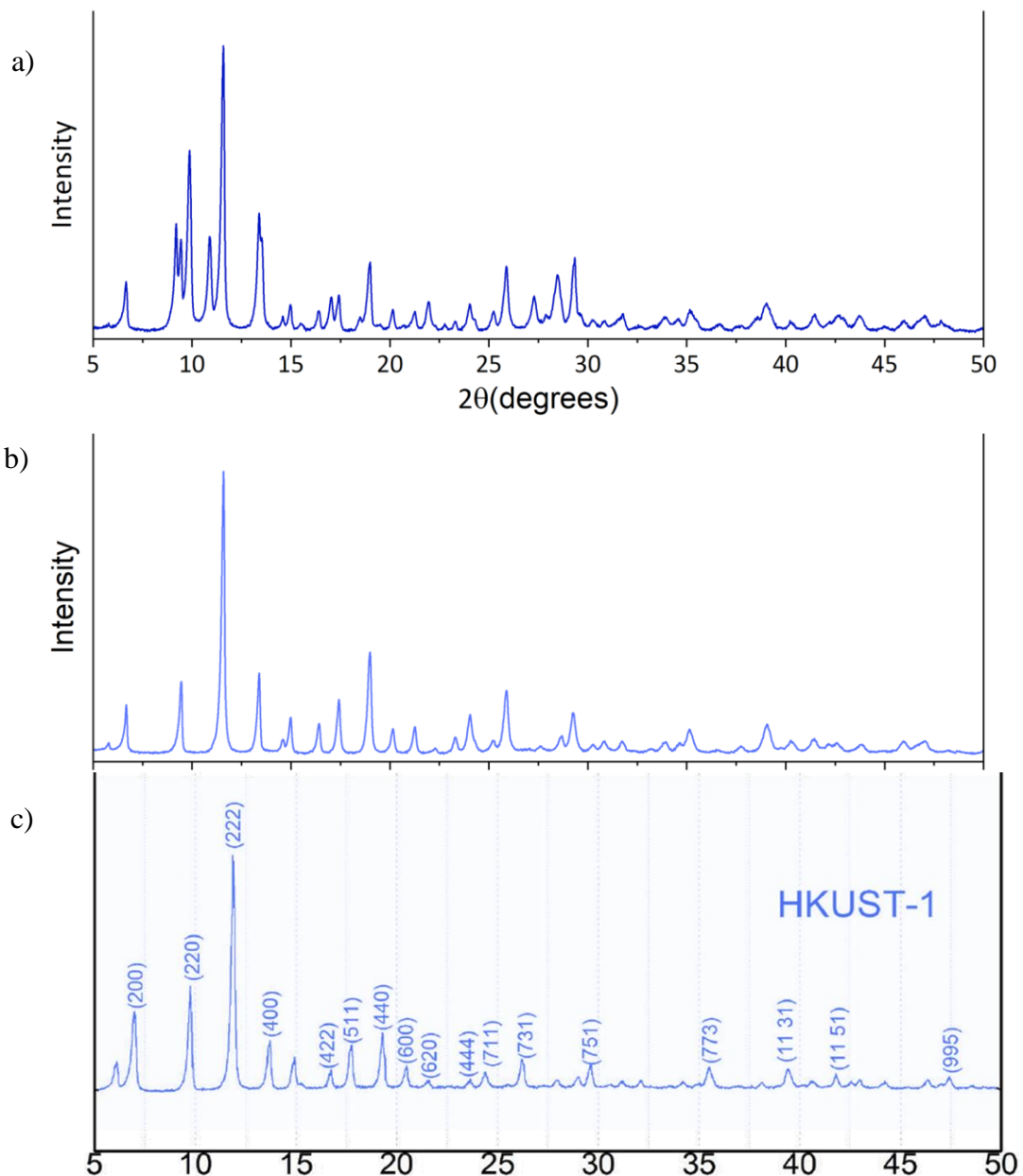

Figure 12. *UV-Vis spectrum of the as-synthesized HKUST-1*

The diffuse reflectance UV-vis spectrum of the obtained material was recorded. The maximum is found at 730 nm, corresponding to the d-d transition of Cu(II). This wavelength of absorption is typical of HKUST-1 as confirmed by literature where this transition usually found in a range of 714 to 729 nm.[54] This value can slightly change depending on what is coordinated on the Cu(II) sites, but such values usually observed when ethanol and water are present[50]. The activated one (after thermal treatment) usually shows a hypsochromic shift but is difficult to record without a closed-cell as water would coordinate to the material within seconds.[50]

4.1.3 N$_2$ adsorption

The N$_2$ adsorption of the material was recorded at the Laboratories of Chemical Engineering Faculty at Universidad Central del Ecuador and showed a low specific surface of 36,7 m^2/g. The specific surface of synthesized can vary enormously in a range of 500-1500 m^2/g depending on the conditions of synthesis.[28] However, our shallow value might reflect an insufficient pre-treatment of the MOF, which probably was inadequate to measure the real porosity of the material. Thus, the pre-treatment was only 30 minutes using He flow, but, the conditions were fixed and could not be changed. Comparing to literature, this pre-treatment seems irrelevant. In consequence, other technics might be required to determine the real surface area of this material without the above mentioned experimental limitations.

4.1.4 X-Ray diffraction

Figure 13. XRD difractogram of the as-synthesized HKUST-1 a) non washed b)washed with ethanol c)from literature

Both the XRD spectra of the synthesized material and the same material washed with ethanol four times have recorded. On the non washed material, many more peaks of diffraction are observed corresponding to the coordination of different reagents of the synthesis. However, when comparing with washed materials, the XRD pattern with literature, it finds a very close match. This

XRD pattern is well known and is characteristic of HKUST-1 material.[1,50] Moreover we can deduce the different Miller index of each peak observed.

Table 4. Calculation of Miller index corresponding to each peak of XRD

2θ	sin²θ	λ*h,k,l	integer	h²+k²+l²	Miller index of planes h,k,l	a	Miller plane
5,9	0,0026	3,072	3	3	111	25,9146	100
6,8	0,0035	4,08	4	4	200	25,9668	110
9,6	0,007	8,122	8	8	220	26,0271	111
11,8	0,0106	12,257	12	12	222	25,9489	200
13,5	0,0138	16,025	16	16	400	26,2044	210
15,1	0,0173	20,026	20	19	331	25,5447	211
17,6	0,0234	27,149	27	27	511	26,153	220
19,2	0,0278	32,262	32	32	440	26,1187	221
20,2	0,0307	35,674	36	36	600	26,3448	310
21,4	0,0345	39,988	40	40	620	26,2293	311
24,2	0,0439	50,97	51	51	551	26,2329	222
26	0,0506	58,699	59	59	731	26,2923	320
28,8	0,0618	71,742	72	72	822	26,2723	321

Additionally, the diffractogram shows narrow peak meaning a high crystallinity of the synthesized compound

4.1.5 Scanning Electrond Microscopy
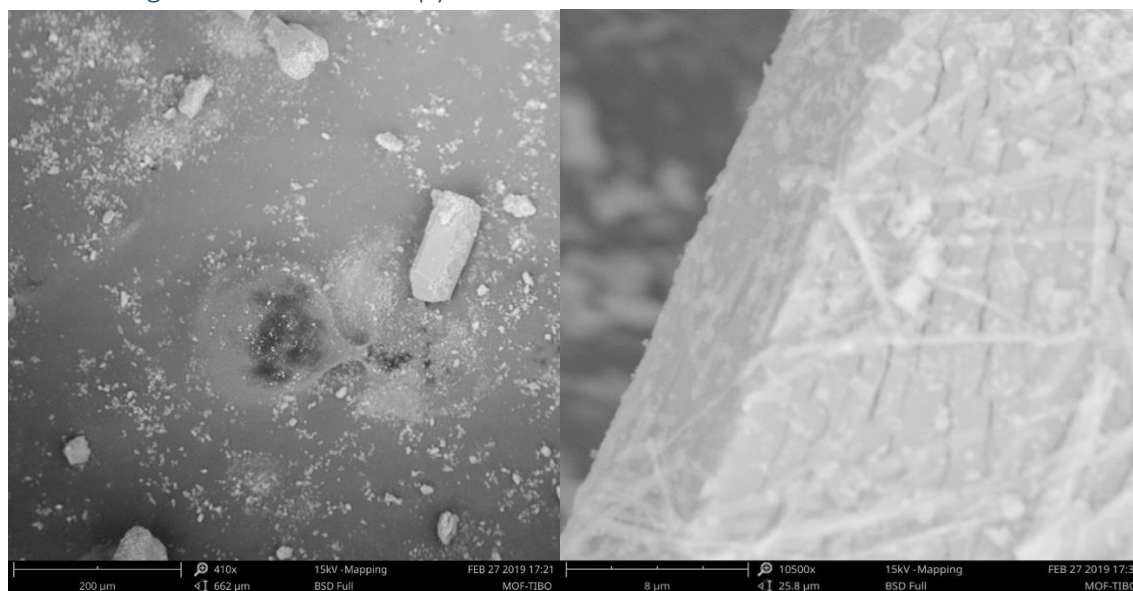
Figure 14. Scanning Electron Microscopy of the as-synthesized HKUST-1 at zoom 410x (left) and 10500x (right)

The scanning electron microscopy of HKUST-1 (**Figure 14**) shows a material with high crystallinity, forming octahedral crystals characteristic of HKUST-1.[55]

4.2 HKUST-1 Ni-doped

4.2.1 Synthesis methods

To dope the Cu-BTC with nickel was used three *methods ship in bottle, bottle around the ship, and one-step*. The first two methods consist of post-synthesis doping that the nickel NPs could be placed in the porosity or the surface of the MOF, and the *one-step* approach is in-situ method; the nickel atoms could replace one or two atoms of copper in the cluster of Cu-BTC or place in the surface or porosity. In the post-synthesis methods, 10% wt of Ni NPs are doping, meanwhile in the in-situ method Ni^{2+} 10% molar replace Cu^{2+} molar quantity.

Synthesis method I: "Ship in Bottle"
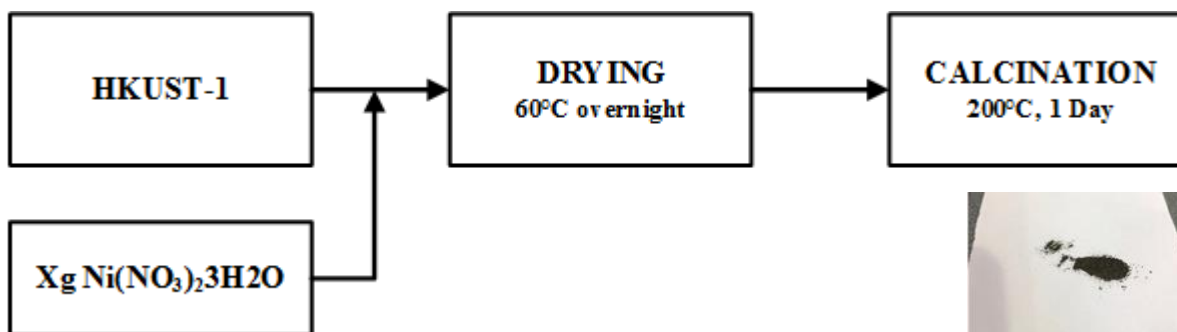
Figure 15. Schematic description of the Synthesis method I: "Ship in Bottle"

1. *Thermal activation:* Before impregnation, the HKUST-1 was activated to eliminate water present in the pores and leave copper II sites free. The samples were activated at 398K for two hours; except to 50%wt samples that were activated under vacuum.[56]
2. *Nickel NPs precursor preparation*: 10% wt $[Ni^{2+}]$ (nickel nitrate as a precursor) was dissolved in 10 mL of ethanol.
3. *The Addition of NPs precursor:* The solution was added gradually drop by drop in the Cu-BTC solid
4. *Drying:* At 323K for 12 hours
5. *Calcined:* at 373 K for 24 hours[57,58]

Synthesis method II: "Bottle Around the Ship"

Figure 16. Schematic description of the Synthesis method I: "Bottle Around the Ship"

1. *Synthesis of Nickel Nanoparticles:* $NiCl_2 \cdot 3H_2O$ was mixed with hydrazine ($N_2H_4/Ni^{2+}=10$) alcohol and KOH ($Ni^{2+}/KOH=10$) as the catalyst for three hours until the mix becomes black. The product was washed with acetone and ethanol four times and dried at 60°C overnight.[59–64]
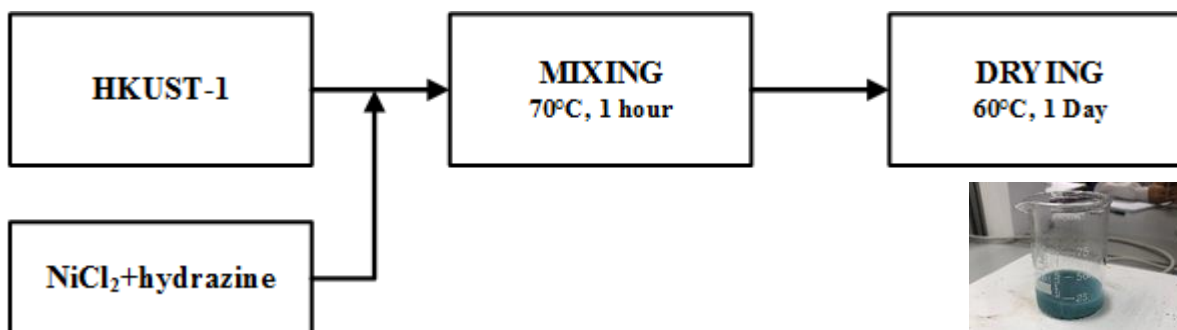
2. *Impregnation*: 10%wt Ni NPs and Cu-BTC was added to 25 mL of ethanol, mixed and heated at 70°C for two hours. Dried at 60°C overnight.

Synthesis method III: "One-Step"
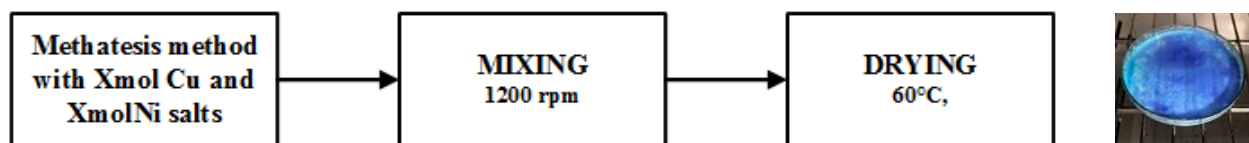
Figure 17. Schematic description of the Synthesis method III: "One-step"

Basing on other procedures, we introduce 10% molar Ni^{2+} to replace Cu^{2+}.[35,41] The procedure was however adapted to our metathesis MOF synthesis method.

1. *Organic linker preparation:* 2.0 mmol (0.25 g) of BTC and 0.35 g of $NaHCO_3$ was dissolve into 100 mL of deionized water: this solution was stirred for one hour.
2. *Precursor salt:* 3.0 mmol (0.3844g) of copper nitrate hexahydrate and 0.23 mmol (0.0665g) of nickel nitrate trihydrate was dissolved in 20 mL of ethanol.
3. *Mixture*: Precursor salt was added gradually drop by drop into the first solution. The mixture was stir at room temperature for 12 hours.

4. *Separation and drying:* The solution was separated by centrifugation, washing three times with ethanol and drying at 373K for 4 hours and 333K for 8 hours.

4.2.2 Nickel nanoparticles characterization

In the synthesis method II, "*Bottle Around the Ship*," the nanoparticles are done before the synthesis of the doped material. In order to assure the success of the synthesis, XRD technic have used (**Figure 18**).
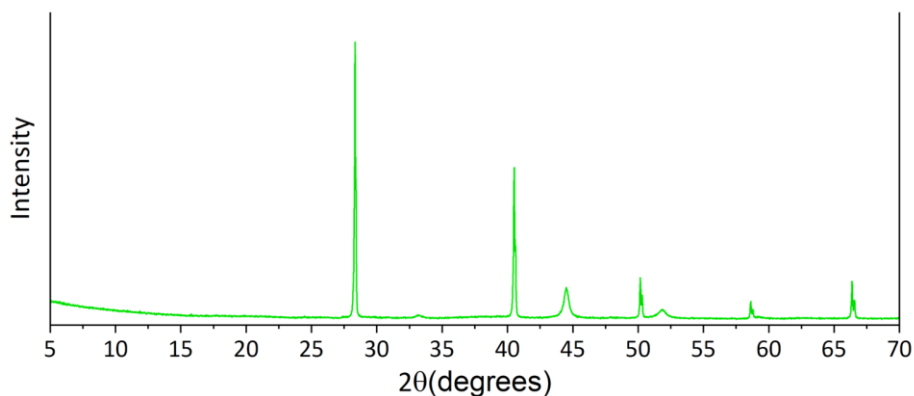
Figure 18. XRD diffractogram of the nickel nanoparticles synthesized following the procedure described before

We can make a direct comparison of the diffractogram with the one measured in the work describing the synthesis method[59]. We can attribute the peaks at angles 44.5, 52 y 77 to the nickel nanoparticles of size 50 nm based on previous work.[59] The relatively narrow peaks reflect a narrow distribution of particle size. With the help of Dr. Edward Avila, all the other narrow peaks could be attributed to the KCl diffraction pattern called Sylvite. The occurrence of KCl is logic due to the presence of both K^+ (from KOH) and Cl^- (from nickel chloride). To conclude this part, we can affirm that the synthesis of nickel nanoparticles was successful.

4.2.3 UV-vis characterization of the obtained material

The diffuse reflectance UV-vis spectrum of the doped materials was recorded. (**Figure 19**)

	SAMPLE	%Ni	METHOD	λmax (nm)
	HKUST-1	0	Solvotherm	**714-29**
	HKUST-1	0	Metatesis	**730**
	HKU-OE-TA	10	one-step	**722**
	HKU-1-TA	10	Impregnat.	**708**
	HKU-2-150	10	Impregnat.	**706**
	HKU-3	50	Impregnat.	**695**
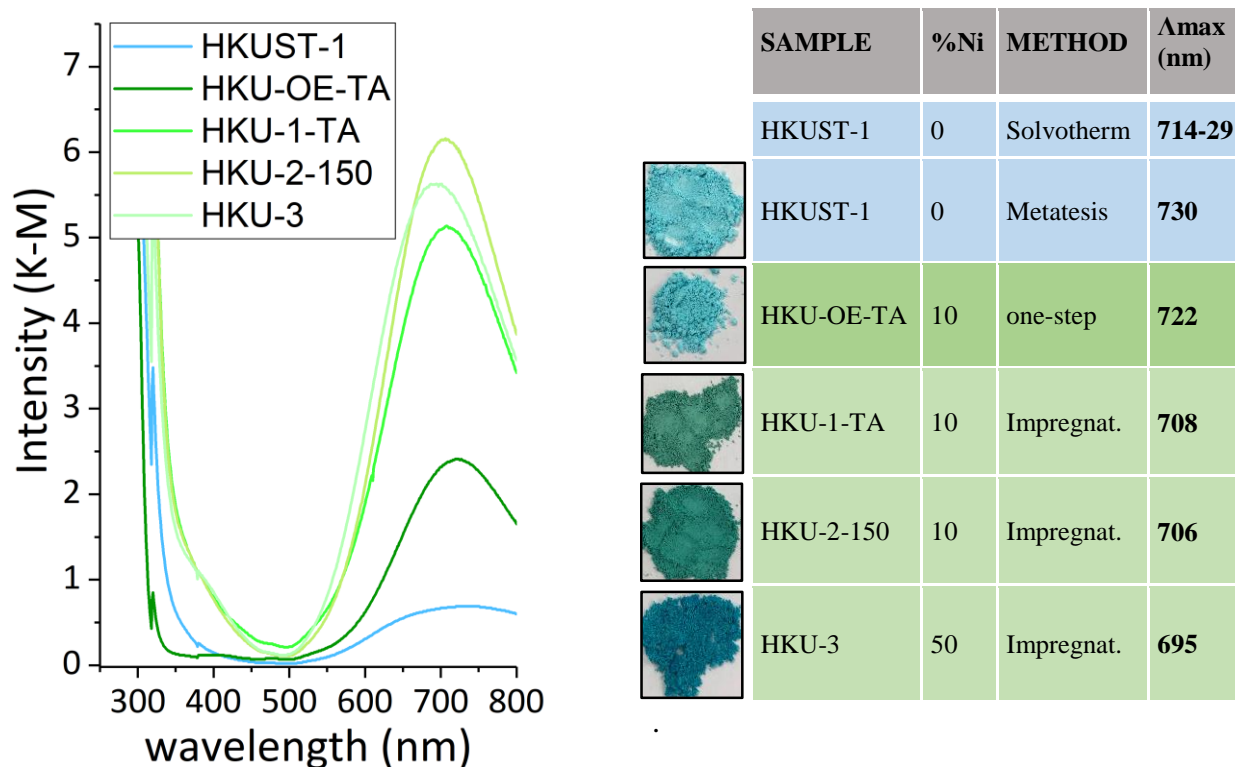
Figure 19. UV-Vis spectra of HKUST-1 (blue) and HKUST-1 doped with Ni through different methods (green)

The maximum corresponding to the d-d transition of Cu(II) undergoes a bathochromic shift for all Ni-doped materials, with a maximum shift of 35 nm for the sample HKUST-3. Nevertheless, no new bands observed in the whole visible range. The logic conclusion is that Nickel is affecting the copper coordination sphere and should be coordinated or close to the copper atom. Comparing between 0%, 10%, and 50%, it seems that the shift becomes more critical with an increasing quantity of Nickel inside the material, suggesting that more Nickel would affect the copper more.

4.2.4 X-Ray diffraction

Figure 20. XRD diffractogram of the Ni-doped HKUST-1 synthesized via in-situ method

The diffractogram for the Ni@HKUST-1 shown in **Figure 20**. The pattern obtained is very similar to the non-washed HKUST-1 sample with some changes in relative intensities. However, these changes are difficult to relate to a significant change of structure. This trend was also viewed in one of the very few similar work[41] where no changes were observed upon the addition of nickel to the MOF. It would suggest that either replacing Cu with Ni do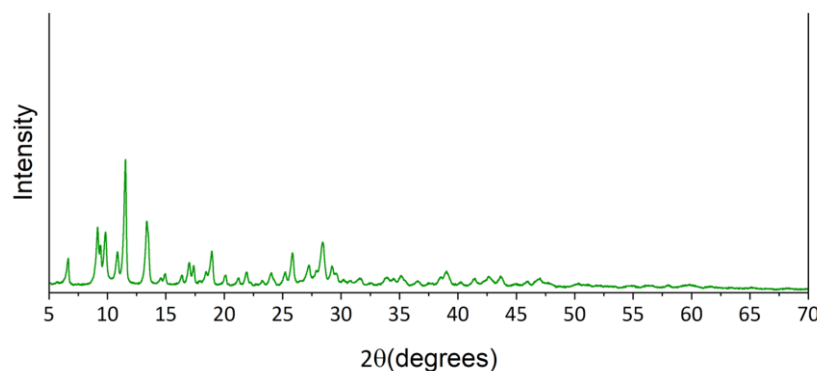es not have any effect on the structure or that the structure is unaffected by the addition of nickel. In order to solve this question, other characterization technics need to be used.

4.2.5   Scanning Electron Microscopy

Scanning electron microscopy of the nickel impregnated HKUST-1 (Figure 21) allows see the crystals of HKUST-1 but also a fluffy cover due to the addition of nickel. This technic allows confirming the presence of nickel at least on the surface of the MOF crystals.
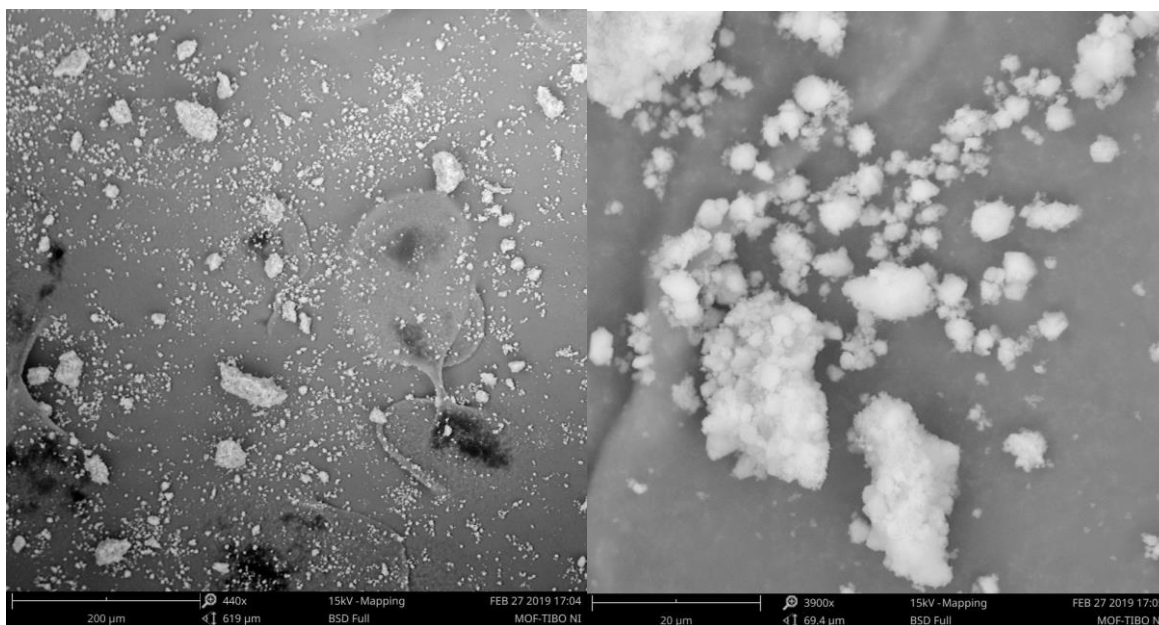
Figure 21: Scanning Electron Microscopy of the Ni-doped HKUST-1 via impregnation at zoom 440x (left) and 3900x (right)

4.2.6   Time-Dependent Density Functional Theory calculation

This part of the theoretical calculations was made using Orca. The most stable structure of the paddlewheel complex (geometry optimization) was calculated using a B3LYP with 6-31G* basis-set. The standard paddlewheel complex containing two copper atoms was used in comparison with a complex containing one Cu and one Ni or two nickel metallic centers. On these minima,

TDDFT calculation allowed to calculate the electronic transitions between the different energy levels and thus deduce the UV-Vis simulated spectra. (Figure 22)
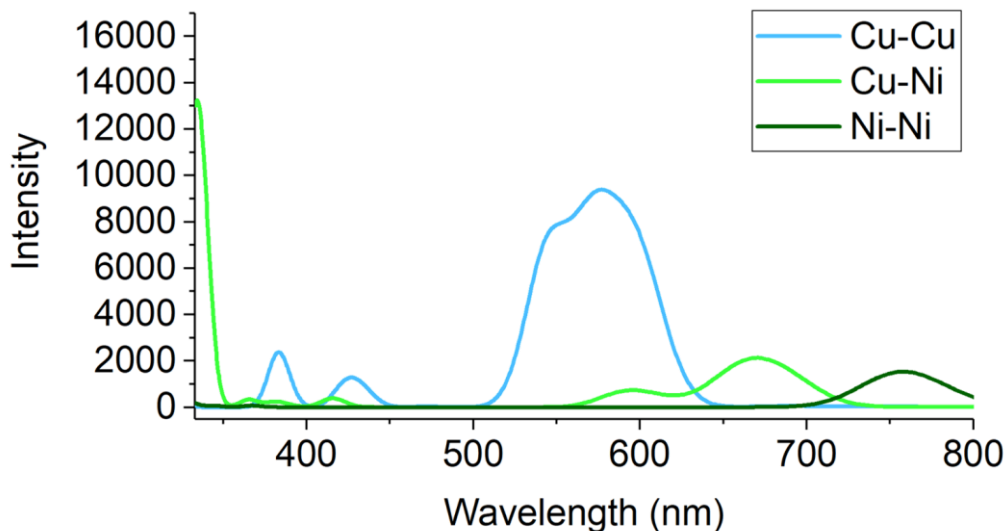
Figure 22. Three simulated UV-vis spectra, using TDDFT method, of the normal paddlewheel complex, of the complex containing one copper and one nickel, and of the complex containing two nickel with water coordinated to the metal centers

One remark is that the copper complex is profoundly shifted from the experimental value. This discrepancy has two sources: 1. the calculation is done with a reasonably poor basis-set 2. The calculation is done only on a representative cluster and not the entire material. From these preliminary calculations, only a qualitative tendency could be deduced. With the addition of nickel, the transitions should undergo a strong bathochromic shift, which is not observed recently.

4.2.7 Where is the Nickel?

Hypothetically, the Nickel could either take the place of copper, remains inside the porosity, remains onto the surface or not be present at all. The Scanning Electron Microscopy confirms the presence of Nickel in the material, eliminating the last possibility.

UV-vis spectra suggest a small shift of the Cu (II) transition without the appearance of another band corresponding to Nickel. It is challenging to conclude solely from UV-Vis spectra, as the characteristic band of Cu (II) is unusually wide and could cover another one. The only information that can be obtained from UV-vis measurements is that a change occurs near copper atoms.

The XRD is very similar between the non-washed material and the doped material. It can only be concluded that the structure, in general, is not or only slightly affected by Ni-doping. However, since the radius of copper and Nickel are similar, it is possible that Nickel incorporates inside the structure without noticeable changes.

With the help of theoretical chemistry (TDDFT method), it is possible to simulate the UV-vis spectrum of the copper and nickel material. The results suggest that, upon Nickel incorporation, a substantial bathochromic shift should occur. Since this change has not observed, one can conclude that Nickel is not incorporating inside the framework but rather inside the porosity or on the surface. The little shift in experimental UV-vis tends to suggest that the Nickel is present in the porosity. As a suggestion, Nitrogen adsorption would bring further argument on that point: if nickel is present inside the porosity, the specific area should decrease. However, as exposed before, the pre-treatment was insufficient and independent of the will, but it would be a way to be sure in the future.

4.3 Catalytic application: benzene oxidation

4.3.1 Reaction test

The direct hydroxylation of benzene to phenol with Cu-BTC based materials as catalyst and H_2O_2 as a source of oxygen have done. The reaction temperature was 273 K, atmospheric pressure, stirred at 50-200 rpm, and the time of reaction depending on the catalyst; in which the solution turns black, that means the complete oxidation of reaction. (**Figure 23**)
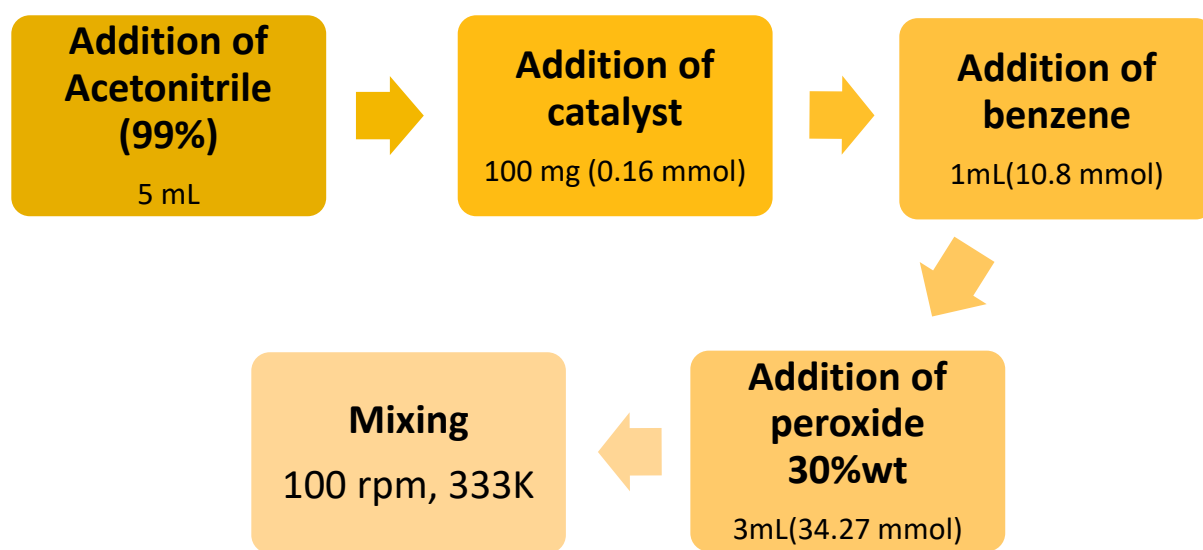
Addition of Acetonitrile (99%) 5 mL	→	Addition of catalyst 100 mg (0.16 mmol)	→	Addition of benzene 1mL(10.8 mmol)

Mixing
100 rpm, 333K

← Addition of peroxide 30%wt
3mL(34.27 mmol)

Figure 23. *Diagram of the procedure followed for the catalytic test.*

4.3.2 Mechanism and diagram of the reaction

The reaction follows the diagram as shown in **Scheme 6**, where the first product formed is phenol, but the problem of this reaction is the overoxidation of phenol and the formation of Quinone, Hydroquinone, and Catechol as byproducts. It means the complete oxidation for the reaction and the reason of the black color of the solution at the end.
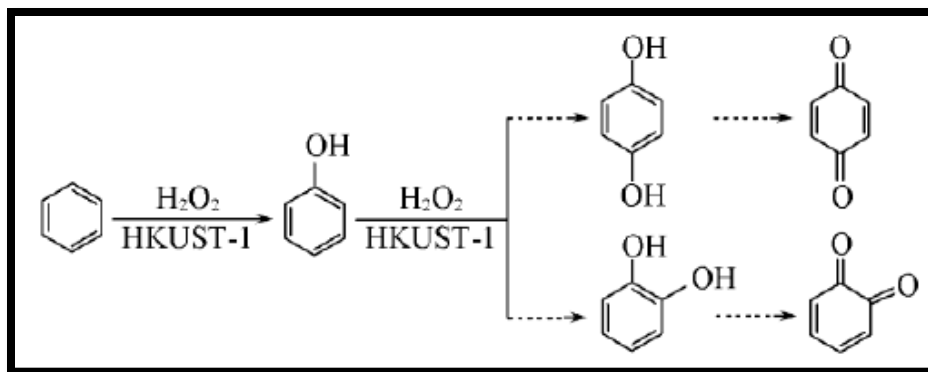
Scheme 6. *Schematic view of benzene oxidation possible products with HKUST-1 (phenol, hydroquinone, benzoquinone)*

The direct hydroxylation of benzene to phenol with H_2O_2 as a source of oxygen is a bimolecular reaction, where the Langmuir-Hinshelwood mechanism could be the more feasible way that this reaction follows. The reaction of benzene adsorbed in the catalyst and the rate-limiting step is the irreversible reaction of the adsorbates:

$$H_2O_2(l) + S \leftrightarrow H_2O_2 - S \quad \text{(Quasi-equilibrium)}$$

$$B(l) + S \leftrightarrow B - S \quad \text{(Quasi-equilibrium)}$$

$$H_2O_2 - S + B - S \rightarrow Phenol + byproducts$$
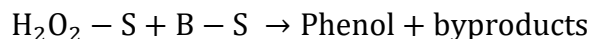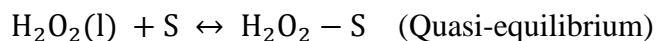
The steps for the catalysis are:

i. Diffusion of the benzene and H_2O_2 in the acetonitrile solvent that surrounds the Cu-BTC solid grain; external diffusion.
ii. Diffusion of benzene and H_2O_2 in the network of the MOF, until the surface of the active sites, Cu^{2+}, Ni^{2+}, and Ni^0; internal diffusion.
iii. Diffusion on the surface include:

    a. Adsorption of the reactants.

    b. Reaction (hydroxylation of benzene).

    c. Desorption of phenol and byproducts.

  iv. Diffusion on the surface

  v. Diffusion of benzene and H_2O_2 in the network.

  vi. Diffusion of the products to the external surface; external diffusion.
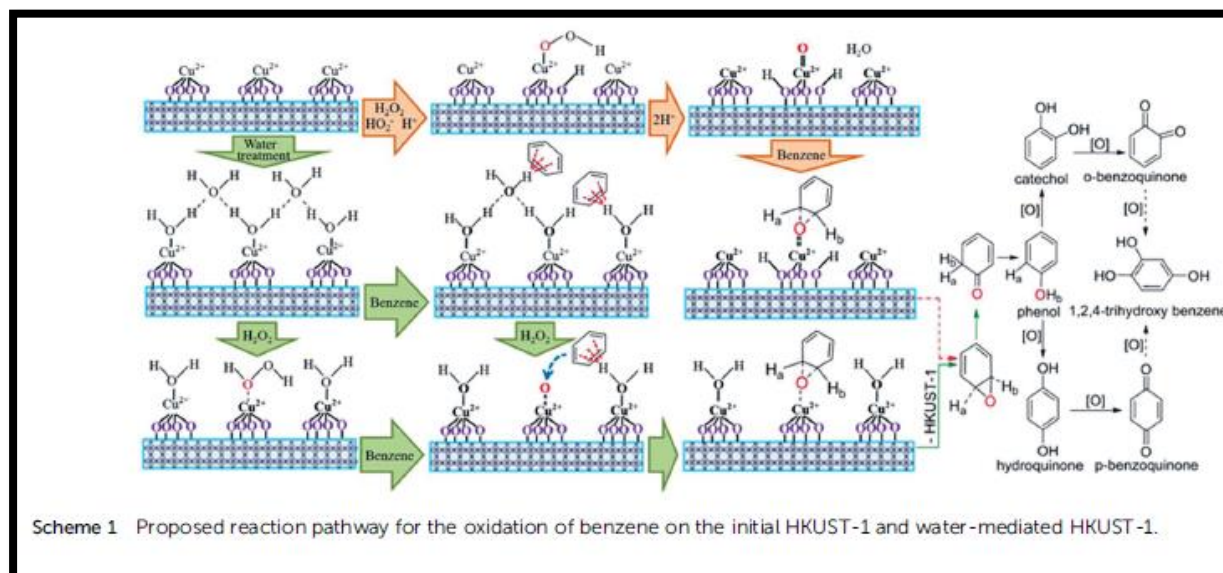

Scheme 1 Proposed reaction pathway for the oxidation of benzene on the initial HKUST-1 and water-mediated HKUST-1.

Scheme 7. Mechanism proposed for the direct hydroxylation of benzene to phenol with HKUST-1 as catalyst and H2O2 as source of hydrogen. [46]

Scheme 7 shows the mechanism proposed by Liu et al,[46] for the direct hydroxylation of benzene with hydrogen peroxide in the presence of Cu-BTC as the catalyst. This scheme clearly shows the conversion of benzene to phenol and byproducts, the mechanism of chemisorption of oxygen and benzene in the metal sites, and how the presence of water affects the sorption of reactants in the metal sites.

4.3.3 Description of the equipment used in the catalytic test.

4.3.4 HKUST-1 as catalyst

  The reaction has done with the procedure described before using non-modified HKUST-1 as synthesized. We followed the reaction over time until complete reaction (i.e, no further evolution in the UV-vis spectrum). For each time, 0.1 ml of the reaction mixture is taken and diluted with 0.8 ml of Acetonitrile. Without this dilution, the species are highly concentrated for recording by

the UV-vis method and would saturate the detector. (**Figure 24**) Different dilutions have tried, but the optimal intensities have found for this dilution.
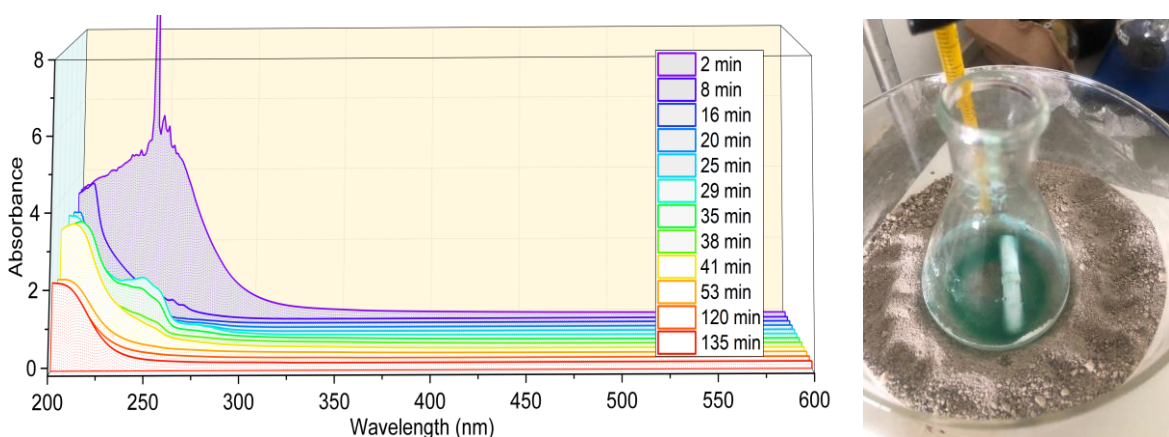
Figure 24. UV-Vis spectra recorded for samples taken at different reaction time of the oxidation of benzene with HKUST-1 catalyst (left) and the end reaction medium transparent (right)

At first glance, the absorption bands observed differ through time and are a reflection of the evolution of the reaction occurring. However, how to identify which ones are present? The approach to distinguish the products of the reaction based on three aspects: 1) comparison with pure species spectrum, 2) literature, and 3) observations. The first one is the privileged one, but it is possible only if it is disposing of the pure species. The second approach proved to be difficult due to the differences in conditions and solvent used for recording the UV-Vis spectra. It is, however, useful in conjunction with the third approach of the observations.

The first approach was useful for the determination of benzene and phenol inside the mixture; both of them were available and have recorded in the UV-vis apparatus. The peaks observed for 188.87, 202, and 254nm for benzene and 190, 217, and 271 nm for phenol. At the beginning of the catalytic test, the multiple peaks at 250 nm clearly confirm the presence of benzene in the reaction medium. The presence of these bands disappear at around 35 minutes. While the reaction continues, other characteristics peaks of phenol appear. The other pure products (hydroquinone and benzoquinone) being not available to us, we needed to follow the other approach.

Figure 25: Fluorescence of the last sample of reaction at 135 min under the UV lamp.

Two key observations have done during the catalytic test: approaching the completion of the reaction, it turns to dark brown, around the middle of the reaction appears a fluorescence in a UV lamp. Bibliographical research confirms both the fluorescence of hydroquinone[65] and the brown color attributed to benzoquinone[46] as well as UV band wavelengths.[66]

Which products are present?

Table 5. Attribution of the different products formed over time and their most characteristic transition

Product	Wavelength (nm)	Time observed (min)
Benzene	250	0-35
Phenol	271	25-40
Hydroquinone	209	30-135
Benzoquinone	240	---

From these approaches, it is possible to make the attribution of the different peaks observed overtime during the catalytic oxidation of benzene. The oxidation of benzene occurs but is not selective only to phenol however undergoes super-oxidation until the hydroquinone. One interesting point is that, under these conditions of reaction, the hydroquinone is selectively formed; meanwhile, the benzoquinone is not formed. The key factor explaining this seems to be if the system (the Erlenmeyer is closed in the top) is open (hydroquinone only) or closed (oxidation until benzoquinone).

4.3.5 Ni-doped HKUST-1 as catalyst for benzene oxidation

The reaction has done with the procedure described before using the Ni-doped HKUST-1 catalyst. Where the sample Ni@HKUST-1 correspond to the material obtained from the *one-step synthesis* method, and the sample Ni/HKUST-1 correspond to the material obtained from the *Bottle around the ship* method. The reaction is followed upon increasing time following the same procedure as in the catalytic test with non-modified HKUST-1.

Figure 26. (left) UV-Vis spectra recorded for samples taken at different reaction time of the oxidation of benzene with Ni@HKUST-1 catalyst (right) Final product solution of the complete oxidation of phenol at 58 minutes.
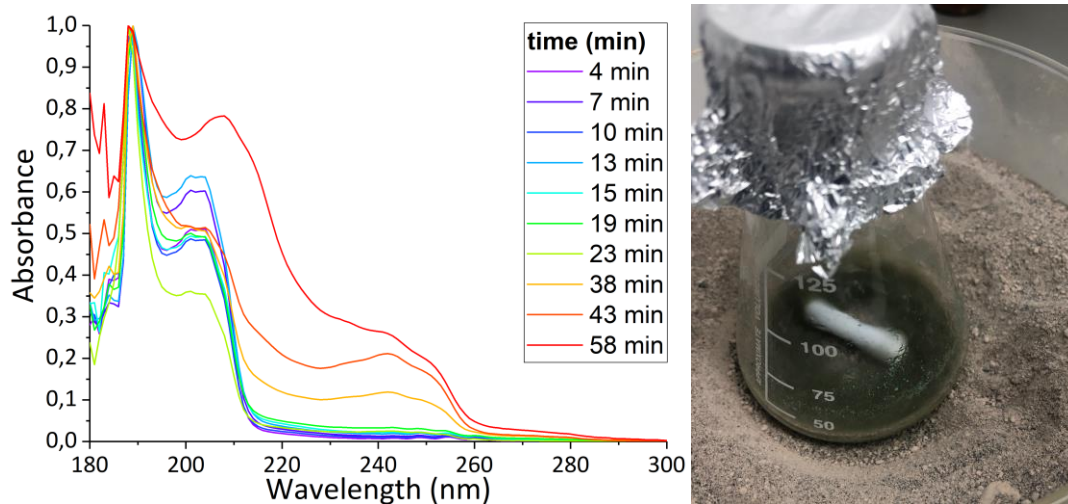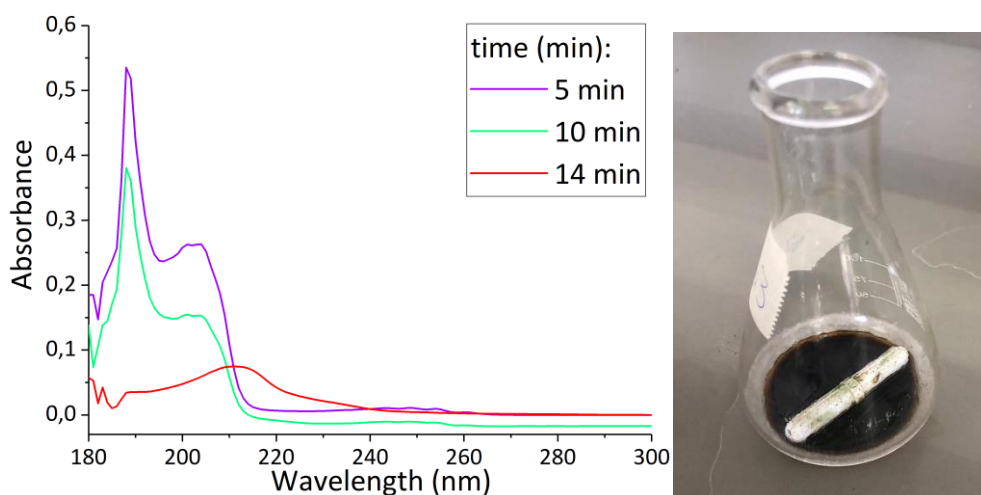

Figure 27. (left) UV-Vis spectra recorded for samples taken at different reaction time of the oxidation of benzene with Ni/ HKUST-1 catalyst (right) Final product solution of the complete oxidation of benzene at 14 minutes.

For the test with Ni@HKUST-1 as the catalyst, the time it takes to complete the total oxidation of benzene was 58 minutes. (Figure 26) The presence of phenol, quinone, and hydroquinone can be seen in the spectrum with their respective peaks, and the dark brown color of the final solution as the indicator of the complete oxidation of phenol. The spectrum shows the presence of benzene in the first runs and the appearance of phenol as the first product of the conversion. The first product of the overoxidation of benzene is the appearance of hydroquinone, and also the presence of quinone as oxidation of hydroquinone.

In the catalytic test using Ni/HKUST-1, the time to complete the total oxidation of benzene decreased significantly to 14 minutes. (Figure 27) The spectrum corroborates the presence of phenol, hydroquinone, and quinone as final products; the final solution presents a dark brown color. In the spectrum, it is visible the presence of hydroquinone and quinone as final products; even the total disappearance of benzene to byproducts.

As a summary, the **Table 6** below presents the time to takes the reaction to reach the complete oxidation of benzene depending on the catalyst used.

Table 6. Time to reach the complete oxidation of benzene depending of the catalyst used in the reaction.

TEST	Time to Complete Oxidation (dark Brown color)
HKUST-1	94 min
Ni@HKUST-1	58 min
Ni/HKUST-1	14 min

4.4 Proposal of Block Diagram Plant using Cu-BTC based materials as catalyst

### 4.4.1 Process selection

This section justifies the reason why the process of direct hydroxylation has chosen and the disadvantages of the other processes.

In the world exists various processes for the production of phenol from benzene as mentioned before; obviously, all of this process has its advantages and disadvantages as shown in **Table7**.

Table 7. Advantages and disadvantages of process for the production of phenol. (obtained from Muhamma et al work)

No	Existing Methods	Raw Materials/ Catalyst	Yield (%)	Products	Comments
1	Cumene Peroxidation	Cumene, air, sulfuric acid, and emulsifying agents.	92	Phenol and acetone	1:1 molar production phenol and acetone
2	Toluene Two-Stage oxidation	Toluene, air, cobalt napthalate, cupric benzoate catalyst.	80	Phenol and carbon dioxide	Low, cost operation by direct toluene application.
3	Rashing Phenol Process	Benzene, air, hydrochloric acid	75	Phenol and hydrochloric acid as recycling.	Feasible under large units.
4	Chlorobenzene caustic hydrolysis	Benzene, chlorine, sodium hydroxide, hydrochloric acid.	95	Phenol, sodium chloride	Economically not feasible
5	Benzene sulfonate process	Benzene, sulfuric acid, sodium hydroxide.	87	Phenol, sodium sulphite, sodium sulphate	Operates on large batch cycle
5	AlphOx Process	Benzene, nitrous oxide, ZSM-5 as catalyst	-	Phenol and nitrogen	High temperatures, availability of nitrous oxide.

For the proposal of BDP, it has been decided to choose the Alphox process, the route of direct hydroxylation of benzene for the production of phenol, being that this process is getting closer to the conditions and step of the reaction. **Figure 28** presents the selection of the technology for this proposal, where the technology is similar, but several operational conditions change to fit the condition of the reaction present in this project as temperature, pressure, and others.
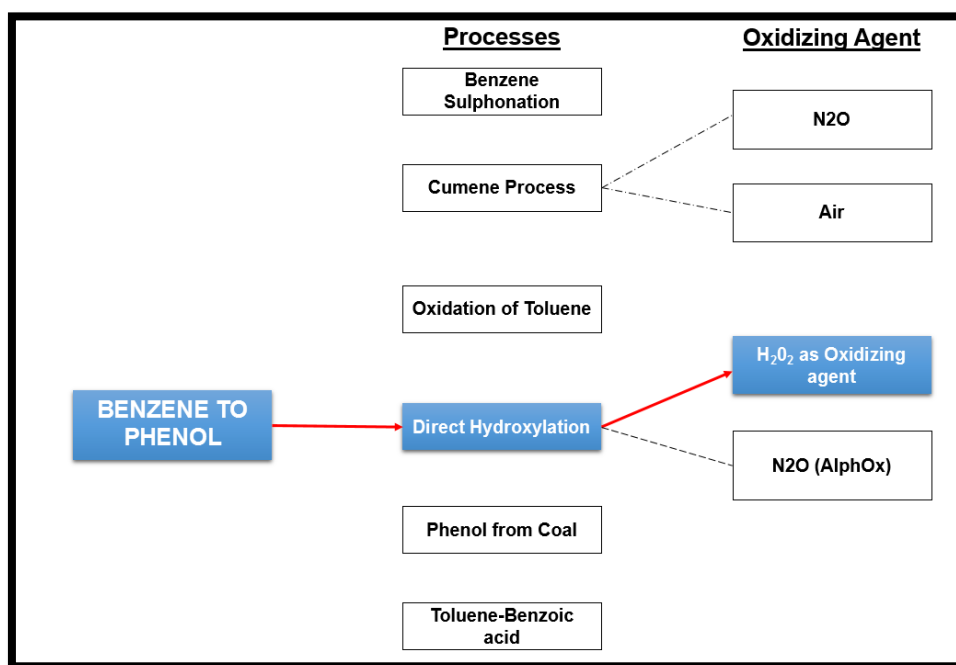
Figure 28. Selection technology for the production of phenol from benzene

The proposal BDP for a plant of direct hydroxylation of benzene to phenol using Cu-BTC based materials as catalyst and H_2O_2 as the oxidizing agent.
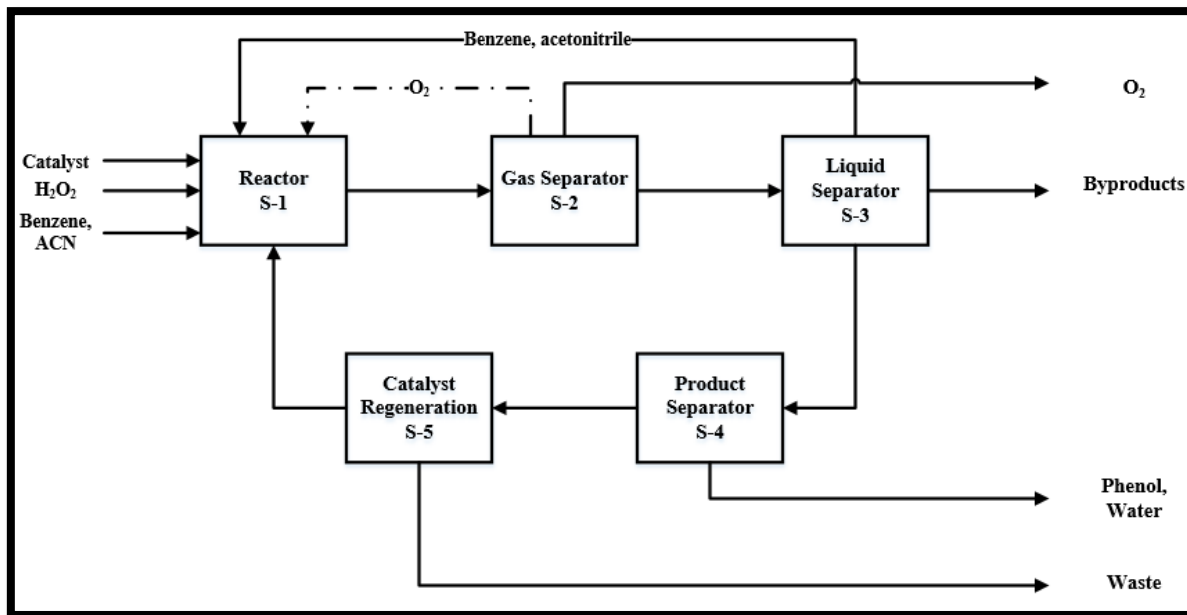
Figure 29. Block Diagram Process proposed for a plant of direct hydroxylation of benzene to phenol using Cu-BTC based materials as catalyst and H_2O_2 as oxidizing agent.

The proposed BDP consists of the feed of the reagents and solvents in the same molar fraction as described before for the catalytic test. The products are phenol, quinone, hydroquinone, water, waste, and oxygen (depending on the final requirements and plant design).

i. **S-1:** *Reactor,* where could be a Continuous Flow Reactor (CFR), where the residence time depending on the catalyst used (HKUST-1, Ni@HKUST-1, Ni/HKUST-1) due to the time to achieve the oxidation and it is different in each one; avoiding the formation of byproducts.

ii. **S-2:** *Gas separator,* consists of the separation of the residual oxygen, could be used as recycling or use for other purposes.

iii. **S-3:** *Liquid separator*, this section focus on the separation of byproducts, acetonitrile, and unreacted benzene through liquid-liquid separation methods. Benzene and acetonitrile return to the reactor.

iv. **S-4:** *Product separator,* consists of the separation of phenol produced, water (residues of hydrogen peroxide), and catalyst.

v. **S-5:** *Catalyst Regeneration,* in this section, the catalyst could receive a treatment to prepare it again to insert in the reactor (S-1), waste or undesired species produced exit of this section.

5 Conclusions

HKUST-1 was successfully synthesized by the metathesis method (in contrast with the usual solvothermal method) and characterized by XRD and UV-vis spectroscopy.

Three methods have used for doping HKUST-1 with nickel to obtain two transition metals as active sites for catalysis, Cu (II) sites of the framework and nickel that could be part of the framework(in-situ) or in the surface or porosity (post-synthesis). TDDFT calculation suggests that the nickel is inside the porous structure rather than making a substitution of copper.

This unprecedented route of synthesis of Ni-doped material presents the main advantage of being possible in very mild conditions in comparison with the common solvothermal process and could be reproduced easily for *in-situ* synthesis of materials doped with other metals

The Ni-doped catalysts synthesized (Ni@HKUST-1 and Ni/HKUST-1 are very active for the direct hydroxylation of benzene but only a low selectivity towards phenol formation indicated by the formation of byproducts such as hydroquinone and quinone.

This work clearly shows that doping HKUST-1 with Nickel is an interesting route towards making a more efficient catalyst for the direct hydroxylation of benzene with hydrogen peroxide as an oxidizing agent at 60°C. However, the critical point of selectivity could be studied further: different conditions can bring different products, avoiding the formation of byproducts, and the over oxidation of phenol. The optimization of the conditions (temperature, time of reaction, and others) for the direct oxidation of benzene could be the subject of future work.

Bibliography

(1) Loera-Serna, S.; Solis, H.; Ortiz, E.; Martínez-Hernandéz, A. L.; Noreña, L. Elimination of Methylene Blue and Reactive Black 5 from Aqueous Solution Using HKUST-1. *Int. J. Environ. Sci. Dev.* **2016**, *8* (4), 241–246. https://doi.org/10.18178/ijesd.2017.8.4.955.

(2) Jessney, B. Joseph Lister (1827-1912): A Pioneer of Antiseptic Surgery Remembered a Century after His Death. *J. Med. Biogr.* **2012**, *20* (3), 107–110. https://doi.org/10.1258/jmb.2011.011074.

(3) DeBono, R.; Laitung, G. Phenolic Household Disinfectants — Further Precautions Required. *Burns* **1997**, *23* (2), 182–185. https://doi.org/https://doi.org/10.1016/S0305-4179(96)00114-3.

(4) Rappoport, Z. *The Chemistry of Phenols*; Wiley: Hoboken, NJ, 2003.

(5) Pilato, L. Phenolic Resins: 100Years and Still Going Strong. *React. Funct. Polym.* **2013**, *73* (2), 270–277. https://doi.org/https://doi.org/10.1016/j.reactfunctpolym.2012.07.008.

(6) Zakoshansky, V. M. The Cumene Process for Phenol-Acetone Production. *Pet. Chem.* **2007**, *47* (4), 273–284. https://doi.org/10.1134/s096554410704007x.

(7) Edward C. M. Chen; Sjobergl, S. L. The Kinetics and Thermodynamics of the Phenol from Cumene Process. *J. Chem. Educ.* **1980**, *57* (6), 458.

(8) Barnicki, S. Synthetic Organic Chemicals; 2012; pp 307–389. https://doi.org/10.1007/978-1-4614-4259-2_10.

(9) Consulting, mechant research &. No Title https://mcgroup.co.uk/news/20140131/global-phenol-supply-exceed-107-mln-tonnes.html.

(10) Cortés-Llerena, C. F. Técnicas Para Mejorar El Transporte de Crudos Pesados Por Oleoductos. **2017**, 139.

(11) Antonio; Barrios, D. *Evaluación y Análisis Preliminar Sobre Plan Maestro de Desarrollo Petroquímico Para Manta (PMPM) Informe Para La Gerencia de Educación Ciencia y Tecnología y La Unidad ZEDE Eloy Alfaro de La Empresa Pública Yachay EP*; 2017.

(12)   Panov, G. I. Advances in Oxidation Catalysis; Oxidation of Benzene to Phenol by Nutrous Oxide. *CATTECH* **2000**, *4* (1), 18–31. https://doi.org/10.1023/A:1011991110517.

(13)   Schmidt, R. J. Industrial Catalytic Processes - Phenol Production. *Appl. Catal. A Gen.* **2005**, *280* (1), 89–103. https://doi.org/10.1016/j.apcata.2004.08.030.

(14)   AKHIR, E. A. B. M. *MINI DESIGN PROJECT (PRODUCTION OF PHENOL)*; 2018.

(15)   Degnan, T. F.; Smith, C. M.; Venkat, C. R. Alkylation of Aromatics with Ethylene and Propylene: Recent Developments in Commercial Processes. *Appl. Catal. A Gen.* **2001**, *221* (1–2), 283–294. https://doi.org/10.1016/S0926-860X(01)00807-9.

(16)   Molinari, R.; Poerio, T. Remarks on Studies for Direct Production of Phenol in Conventional and Membrane Reactors. *Asia-Pacific J. Chem. Eng.* **2010**, *5* (1), 191–206. https://doi.org/10.1002/apj.369.

(17)   Daowdat, B.; Hoeltzel, G. D.; Tannenbaum, R. Direct Route to Phenol from Benzene. *Sr. Des. Reports* **2017**, *98*, 316.

(18)   Khirsariya, P.; Mewada, R. K. Review of Direct Hydroxylation of Benzene To Phenol and Its Thermodynamic Analysis.

(19)   Burke, R. F.; Motard, R. L.; Canjar, L. N.; Beckmann, R. B. The Effect of Catalyst Granule Size on the Hydrogenation of Benzene over a Supported Nickel Catalyst. *J. Appl. Chem.* **1957**, *7* (3), 105–109. https://doi.org/10.1002/jctb.5010070302.

(20)   Bohnet, M. *Ullmann's Encyclopedia of Industrial Chemistry*; Wiley-VCH: Weinheim, Germany, 2002. https://doi.org/10.1002/14356007.

(21)   Zhang, L.; Liu, H. H.; Li, G. Y.; Hu, C. W. Continuous Flow Reactor for Hydroxylation of Benzene to Phenol by Hydrogen Peroxide. *Chinese J. Chem. Phys.* **2012**, *25* (5), 585–591. https://doi.org/10.1088/1674-0068/25/05/585-591.

(22)   Balducci, L.; Bianchi, D.; Bortolo, R.; D'Aloisio, R.; Ricci, M.; Tassinari, R.; Ungarelli, R. Direct Oxidation of Benzene to Phenol with Hydrogen Peroxide over a Modified Titanium Silicalite. *Angew. Chemie - Int. Ed.* **2003**, *42* (40), 4937–4940. https://doi.org/10.1002/anie.200352184.

(23) Notté, P. P. The AlphOx^{TM} Process or the One-Step Hydroxylation of Benzene into Phenol by Nitrous Oxide. Understanding and Tuning the ZSM-5 Catalyst Activities. *Top. Catal.* **2000**, *13* (4), 387–394. https://doi.org/10.1023/A:1009015223793.

(24) Furukawa, H.; Cordova, K. E.; O'Keeffe, M.; Yaghi, O. M. The Chemistry and Applications of Metal-Organic Frameworks. *Science (80-.).* **2013**, *341* (6149). https://doi.org/10.1126/science.1230444.

(25) Topologies, M. O. F.; Stock, N.; Biswas, S. Chem. Rev. 2012, 112, 933–969.Pdf. **2012**, 933–969. https://doi.org/10.1021/cr200304e.

(26) Öhrström, L. Let's Talk about MOFs—Topology and Terminology of Metal-Organic Frameworks and Why We Need Them. *Crystals* **2015**, *5* (1), 154–162. https://doi.org/10.3390/cryst5010154.

(27) Chui, S. S.-Y.; Lo, S. M.-F.; Charmant, J. P. H.; Orpen, A. G.; Williams, I. D. A Chemically Functionalizable Nanoporous Material [Cu3(TMA)2(H2O)3]N. *Science (80-.).* **1999**, *283* (5405), 1148–1150. https://doi.org/10.1126/science.283.5405.1148.

(28) Liu, Y.; Liu, B.; Zhou, Q.; Zhang, T.; Wu, W. Morphology Effect of Metal-Organic Framework HKUST-1 as a Catalyst on Benzene Oxidation. *Chem. Res. Chinese Univ.* **2017**, *33* (6), 971–978. https://doi.org/10.1007/s40242-017-6468-4.

(29) Granato, T.; Testa, F.; Olivo, R. Catalytic Activity of HKUST-1 Coated on Ceramic Foam. *Microporous Mesoporous Mater.* **2012**, *153*, 236–246. https://doi.org/10.1016/j.micromeso.2011.12.055.

(30) Loera-Serna, S.; Ortiz, E. Catalytic Applications of Metal-Organic Frameworks; 2016. https://doi.org/10.5772/61865.

(31) McKinstry, C.; Cussen, E. J.; Fletcher, A. J.; Patwardhan, S. V.; Sefcik, J. Scalable Continuous Production of High Quality HKUST-1 via Conventional and Microwave Heating. *Chem. Eng. J.* **2017**, *326*, 570–577. https://doi.org/10.1016/j.cej.2017.05.169.

(32) Martinez Joaristi, A.; Juan-Alcañiz, J.; Serra-Crespo, P.; Kapteijn, F.; Gascon, J. Electrochemical Synthesis of Some Archetypical Zn2+, Cu2+, and Al3+ Metal Organic Frameworks. *Cryst. Growth Des.* **2012**, *12* (7), 3489–3498.

https://doi.org/10.1021/cg300552w.

(33)   Klinowski, J.; Almeida Paz, F. A.; Silva, P.; Rocha, J. Microwave-Assisted Synthesis of Metal–Organic Frameworks. *Dalt. Trans.* **2011**, *40* (2), 321–330. https://doi.org/10.1039/C0DT00708K.

(34)   Ma, L.; Lin, W. Designing Metal-Organic Frameworks for Catalytic Applications. In *Functional Metal-Organic Frameworks: Gas Storage, Separation and Catalysis*; Schröder, M., Ed.; Springer Berlin Heidelberg: Berlin, Heidelberg, 2010; pp 175–205. https://doi.org/10.1007/128_2009_20.

(35)   Abd El Salam, H. M.; Zaki, T. Removal of Hazardous Cationic Organic Dyes from Water Using Nickel-Based Metal-Organic Frameworks. *Inorganica Chim. Acta* **2018**, *471*, 203–210. https://doi.org/10.1016/j.ica.2017.10.040.

(36)   Lee, J.; Farha, O. K.; Roberts, J.; Scheidt, K. A.; Nguyen, S. T.; Hupp, J. T. Metal-Organic Framework Materials as Catalysts. *Chem. Soc. Rev.* **2009**, *38* (5), 1450–1459. https://doi.org/10.1039/b807080f.

(37)   Yang, D.; Gates, B. C. Catalysis by Metal Organic Frameworks: Perspective and Suggestions for Future Research. *ACS Catal.* **2019**, *9* (3), 1779–1798. https://doi.org/10.1021/acscatal.8b04515.

(38)   Kim, H. K.; Yun, W. S.; Kim, M.; Kim, J. Y.; Bae, Y.; Lee, J. A Chemical Route to Activation of Open Metal Sites in the Copper-Based Metal–Organic Framework Materials HKUST-1 and Cu-MOF-2 - Journal of the American Chemical Society (ACS Publications). *222* (v), 1–8.

(39)   Yepez, R.; García, S.; Schachat, P.; Sánchez-Sánchez, M.; González-Estefan, J. H.; González-Zamora, E.; Ibarra, I. A.; Aguilar-Pliego, J. Catalytic Activity of HKUST-1 in the Oxidation of Trans-Ferulic Acid to Vanillin. *New J. Chem.* **2015**, *39* (7), 5112–5115. https://doi.org/10.1039/c5nj00247h.

(40)   Schlichte, K.; Kratzke, T.; Kaskel, S. Improved Synthesis, Thermal Stability and Catalytic Properties of the Metal-Organic Framework Compound Cu3(BTC)2. *Microporous Mesoporous Mater.* **2004**, *73* (1–2), 81–88.

https://doi.org/10.1016/j.micromeso.2003.12.027.

(41)   Safii, F. F.; Ediati, R. Synthesis Of Nickel (Ni) Doped HKUST - 1 Using Solvotermal Method with Addition of Acetic Acid as Modulator. **2015**, 163–164.

(42)   Li, H.; Shi, W.; Zhao, K.; Li, H.; Bing, Y.; Cheng, P. Enhanced Hydrostability in Ni-Doped MOF-5. *Inorg. Chem.* **2012**, *51* (17), 9200–9207. https://doi.org/10.1021/ic3002898.

(43)   Hu, J.; Yu, H.; Dai, W.; Yan, X.; Hu, X.; Huang, H. Enhanced Adsorptive Removal of Hazardous Anionic Dye "Congo Red" by a Ni/Cu Mixed-Component Metal-Organic Porous Material. *RSC Adv.* **2014**, *4* (66), 35124–35130. https://doi.org/10.1039/c4ra05772d.

(44)   Xiang, W.; Zhang, Y.; Lin, H.; Liu, C. J. Nanoparticle/Metal-Organic Framework Composites for Catalytic Applications: Current Status and Perspective. *Molecules* **2017**, *22* (12). https://doi.org/10.3390/molecules22122103.

(45)   Zhao, Z.; Wang, S.; Yang, Y.; Li, X.; Li, J.; Li, Z. Competitive Adsorption and Selectivity of Benzene and Water Vapor on the Microporous Metal Organic Frameworks (HKUST-1). *Chem. Eng. J.* **2015**, *259*, 79–89. https://doi.org/10.1016/j.cej.2014.08.012.

(46)   Liu, Y.; Zhang, T.; Wu, W.; Jiang, S.; Zhang, H.; Li, B. Water-Mediated Promotion of Direct Oxidation of Benzene over the Metal-Organic Framework HKUST-1. *RSC Adv.* **2015**, *5* (69), 56020–56027. https://doi.org/10.1039/c5ra05595d.

(47)   Morimoto, Y.; Bunno, S.; Fujieda, N.; Sugimoto, H.; Itoh, S. Direct Hydroxylation of Benzene to Phenol Using Hydrogen Peroxide Catalyzed by Nickel Complexes Supported by Pyridylalkylamine Ligands. *J. Am. Chem. Soc.* **2015**, *137* (18), 5867–5870. https://doi.org/10.1021/jacs.5b01814.

(48)   Yamada, M.; Karlin, K. D.; Fukuzumi, S. One-Step Selective Hydroxylation of Benzene to Phenol with Hydrogen Peroxide Catalysed by Copper Complexes Incorporated into Mesoporous Silica-Alumina. *Chem. Sci.* **2016**, *7* (4), 2856–2863. https://doi.org/10.1039/c5sc04312c.

(49)   Vanoy Villamil, M. N. Deshidratacion Catalitica de D-Xilosa Con Solidos Acidos Para La Produccion de Furfural, Universidad Nacional del Litoral Argentina, 2014.

(50) Terencio, T. Etude de l'adsorption Des COVs Dans Les MOFs Par Une Approche Complémentaire Théorie-Expérience, Ecole Nationale Superieur de Chimie de Montpellier (ENSCM), 2013.

(51) Pachfule, P.; Das, R.; Poddar, P.; Banerjee, R. Solvothermal Synthesis, Structure, and Properties of Metal Organic Framework Isomers Derived from a Partially Fluorinated Link. *Cryst. Growth Des.* **2011**, *11* (4), 1215–1222. https://doi.org/10.1021/cg101414x.

(52) Sun, Y.; Zhou, H.-C. Recent Progress in the Synthesis of Metal–Organic Frameworks. *Sci. Technol. Adv. Mater.* **2015**, *16* (5), 54202. https://doi.org/10.1088/1468-6996/16/5/054202.

(53) Weber Aguiar, L.; Thiago Pereira da Silva, C.; Henrique Carline de Lima, H.; Pereira Moises, M.; Wellington Rinaldi, A. Evaluation of the Synthetic Methods for Preparing Metal Organic Frameworks with Transition Metals. *AIMS Materials Science*. 2018, pp 467–478. https://doi.org/10.3934/matersci.2018.3.467.

(54) Alaerts, L.; Maes, M.; van der Veen, M. A.; Jacobs, P. A.; De Vos, D. E. Metal–Organic Frameworks as High-Potential Adsorbents for Liquid-Phase Separations of Olefins{,} Alkylnaphthalenes and Dichlorobenzenes. *Phys. Chem. Chem. Phys.* **2009**, *11* (16), 2903–2911. https://doi.org/10.1039/B823233D.

(55) Gascon, J.; Aguado, S.; Kapteijn, F. Manufacture of Dense Coatings of $Cu_3(BTC)_2$ (HKUST-1) on α-Alumina. *Microporous Mesoporous Mater.* **2008**, *113* (1), 132–138. https://doi.org/https://doi.org/10.1016/j.micromeso.2007.11.014.

(56) Bao, L.; Li, X.; Wu, Z.; Yuan, X.; Luo, H. N-Hydroxyphthalimide Incorporated onto Cu-BTC Metal Organic Frameworks: An Novel Catalyst for Aerobic Oxidation of Toluene. *Res. Chem. Intermed.* **2016**, *42* (6), 5527–5539. https://doi.org/10.1007/s11164-015-2384-8.

(57) Chandra, S.; Kumar, A.; Tomar, P. K. Synthesis of Ni Nanoparticles and Their Characterizations. *J. Saudi Chem. Soc.* **2011**, *18* (5), 437–442. https://doi.org/10.1016/j.jscs.2011.09.008.

(58) Brockner, W.; Ehrhardt, C.; Gjikaj, M. Thermal Decomposition of Nickel Nitrate Hexahydrate, $Ni(NO_3)_2 \cdot 6H_2O$, in Comparison to $Co(NO_3)_2 \cdot 6H_2O$ and $Ca(NO_3)_2 \cdot 4H_2O$. *Thermochim. Acta* **2007**, *456* (1), 64–68. https://doi.org/10.1016/j.tca.2007.01.031.

(59) Wu, Z. G.; Munoz, M.; Montero, O. The Synthesis of Nickel Nanoparticles by Hydrazine Reduction. *Adv. Powder Technol.* **2010**, *21* (2), 165–168. https://doi.org/10.1016/j.apt.2009.10.012.

(60) Yin, M.; Wu, C.; Lou, Y.; Burda, C.; Koberstein, J. T.; Zhu, Y.; Brien, S. O. 1039.J.Am.Chem.Soc.2005,127,9506.Pdf. **2005**, No. 12, 9506–9511.

(61) BR, S.; XR, J. Effect of Calcination Time on Structural, Optical and Antimicrobial Properties of Nickel Oxide Nanoparticles. *J. Theor. Comput. Sci.* **2017**, *03* (02). https://doi.org/10.4172/2376-130x.1000149.

(62) Eluri, R.; Paul, B. Synthesis of Nickel Nanoparticles by Hydrazine Reduction: Mechanistic Study and Continuous Flow Synthesis. *J. Nanoparticle Res.* **2012**, *14* (4), 1–14. https://doi.org/10.1007/s11051-012-0800-1.

(63) El-Kemary, M.; Nagy, N.; El-Mehasseb, I. Nickel Oxide Nanoparticles: Synthesis and Spectral Studies of Interactions with Glucose. *Mater. Sci. Semicond. Process.* **2013**, *16* (6), 1747–1752. https://doi.org/10.1016/j.mssp.2013.05.018.

(64) Puente-Urbina, B. A.; García-Cerda, L. A.; De León-Quiroz, E. L.; López-Martínez, M. G. Nanopartículas de Ni/NiO y Cu-Ag Obtenidas Mediante El Método de Pechini: Síntesis y Caracterización. *Superf. y Vacio* **2012**, *25* (3), 183–187.

(65) Ravichandiran, P.; Vasanthkumar, S. Synthesis of Heterocyclic Naphthoquinone Derivatives as Potent Organic Fluorescent Switching Molecules. *J. Taibah Univ. Sci.* **2015**, *9* (4), 538–547. https://doi.org/10.1016/j.jtusci.2014.12.003.

(66) Su, R.; Kesavan, L.; Jensen, M. M.; Tiruvalam, R.; He, Q.; Dimitratos, N.; Wendt, S.; Glasius, M.; Kiely, C. J.; Hutchings, G. J.; et al. Selective Photocatalytic Oxidation of Benzene for the Synthesis of Phenol Using Engineered Au-Pd Alloy Nanoparticles Supported on Titanium Dioxide. *Chem. Commun.* **2014**, *50* (84), 12612–12614. https://doi.org/10.1039/c4cc04024d.

Annexes

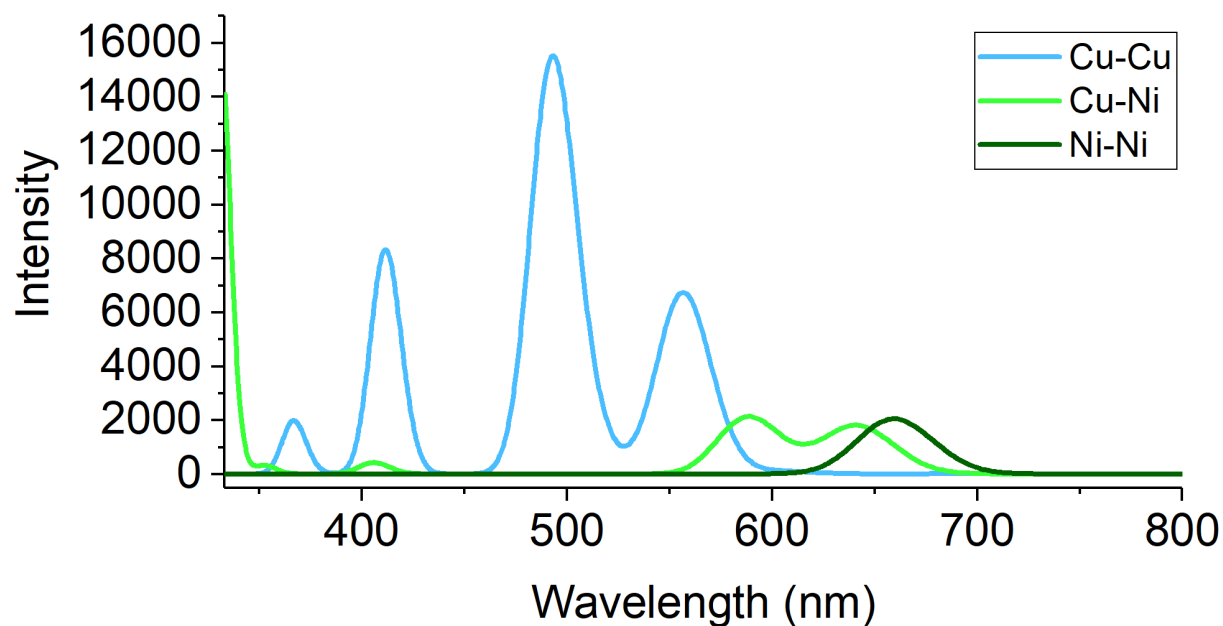## Annex 1

Near-IR spectra of Ni-doped HKUST-1 materials
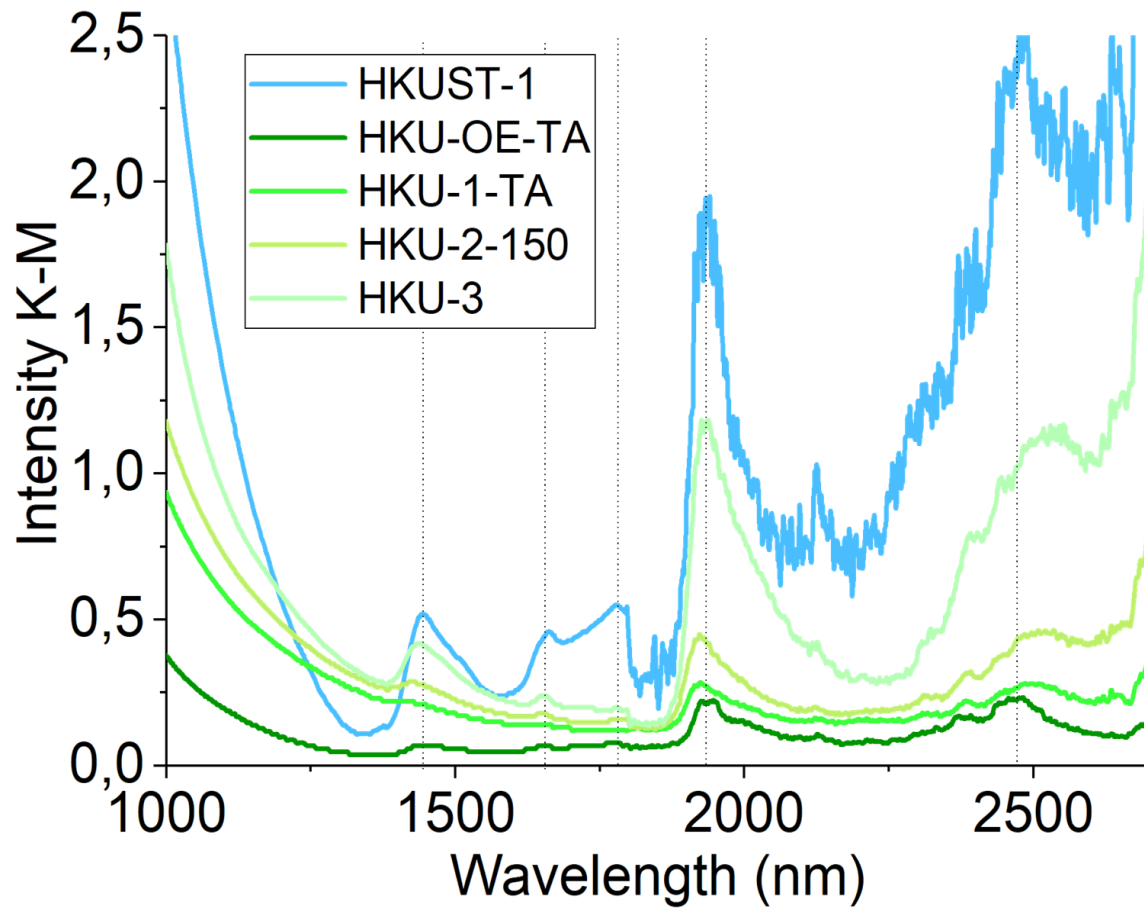
Annex 2

Three simulated UV-vis spectra, using TDDFT method, of the normal paddlewheel complex, of the complex containing one copper and one nickel, and of the complex containing two nickel, without any molecules coordinated to the metal centers.

Annex 3

KCl pattern provided by E. Avila

COD CIF File	http://www.crystallography.net/cod/9008651.html
Mineral Name	Sylvite
Formula	Cl K
Quality	C (calculated pattern)
I/Ic	6.15

Reference	Wyckoff, R. W. G., Crystal Structures, **1** (1963)

Space Group	F m -3 m	(225)
Crystal system	Cubic	
Cell parameters	a=6.2929 Å	
Cell volume	249.21 Å3	
Wavelength	1.54056 Å	
μ (Cu Kα)	251.281 cm-1	

Diffraction data

2theta	d[A]	Int.	hkl	mult
24.4805	3.6332	5.91	1 1 1	8
28.3407	3.1465	1000.00	2 0 0	6
40.5112	2.2249	653.89	2 2 0	12
47.9034	1.8974	3.71	3 1 1	24
50.1777	1.8166	206.91	2 2 2	8
58.6320	1.5732	88.34	4 0 0	6
64.4907	1.4437	0.94	3 3 1	24
66.3809	1.4071	226.24	4 2 0	24
73.6930	1.2845	158.10	4 2 2	24
78.9909	1.2111	0.40	5 1 1	24
87.6485	1.1124	47.40	4 4 0	12
92.7966	1.0637	0.27	5 3 1	48
94.5197	1.0488	100.08	4 4 2	24
101.4562	0.9950	71.18	6 2 0	24
106.7632	0.9597	0.09	5 3 3	24
108.5703	0.9487	66.38	6 2 2	24
115.9995	0.9083	21.61	4 4 4	8
121.8834	0.8812	0.18	5 5 1	24
123.9250	0.8727	66.42	6 4 0	24
132.7016	0.8409	144.17	6 4 2	48
140.1597	0.8193	0.39	7 3 1	48

Physical Properties

Calc. density	1.987 g cm-3

Remarks

Diffraction pattern calculated by EXPO from COD database CIF file
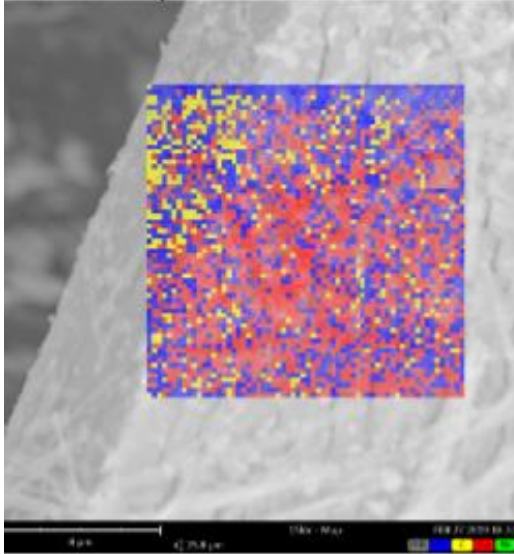I/Ic calcuted by EXPO

Annex 4
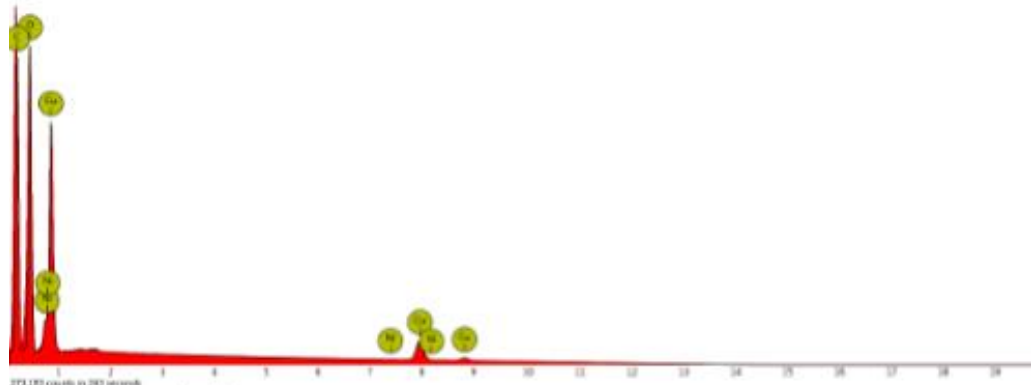
Elemental analysis of SEM image of HKUST-1

Image 2
1. map

Combined map

Element Symbol	Atomic Conc.	Weight Conc.	Oxide Symbol	Stoich. Conc.
O	42.63	45.33		
C	54.77	43.72	C	95.48
Cu	2.59	10.95	Cu	4.52
Ni	0.00	0.00	Ni	0.00

FOV: 25.8 µm, Mode: 15kV - Map, Detector: BSD Full, Time: FEB 27 2019 18:32

Disabled elements: B

Annex 4

Elemental analysis of SEM image of HKUST-1 impregnated with Nickel

Image 6
1. region

Element Symbol	Atomic Conc.	Weight Conc.	Oxide Symbol	Stoich. Conc.
C	66.11	55.14	C	96.73
O	31.66	35.17		
Cu	2.06	9.09	Cu	3.02
Ni	0.12	0.49	Ni	0.18
Si	0.05	0.10	Si	0.08

FOV: 34.3 µm, Mode: 15kV – Map, Detector: BSD Full, Time: FEB 27 2019 18:06

Disabled elements: B